

PREPARATION AND CHARACTERIZATION OF POLY (PROPYLENE FUMARATE)
(PPF) BASED COMPOSITES AS SCAFFOLDS FOR BONE TISSUE ENGINEERING
APPLICATIONS



by
Avram Aruh

Submitted to Graduate School of Natural and Applied Sciences
in Partial Fulfillment of the Requirements
for the Degree of Master of Science in
Chemical Engineering

Yeditepe University

2019

PREPARATION AND CHARACTERIZATION OF POLY(PROPYLENE FUMARATE)
(PPF) BASED COMPOSITES AS SCAFFOLDS FOR BONE TISSUE ENGINEERING
APPLICATIONS

APPROVED BY:

Assoc. Prof. Dr. Erde Can
(Thesis Supervisor)
(Yeditepe University)

Prof. Dr. Duygu Avcı
(Boğaziçi University)

Prof. Dr. Gamze Torun Köse
(Yeditepe University)

DATE OF APPROVAL:/...../2019

ACKNOWLEDGEMENTS

First and foremost, I would like to express my sincere gratitude to my thesis supervisor Assoc. Prof. Erde Can for studying with me in this project and I would like to thank her for unlimited contributions to this project in Yeditepe University. It would not have been possible to complete this thesis without her. Her guidance, motivation, support, knowledge, teachings and advices helped me in all time of writing this thesis.

Besides, I am deeply thankful to my project colleague Görkem Cemali for her help, advices, support and friendship. It was a remarkable experience to work with her.

I would like to thank all of the assistants during my Master's degree study in Chemical Engineering Department. We had so many moments to remember in the future. Especially, I would like to thank Barış Emek for his positive personality, moral support and guidance during my Master's Degree study. It was a unique chance to share an office and working with him. Also, our professors especially, Prof. Dr. Süheyla Uzman, Prof. Dr. Salih Dinçer, Prof. Seyda Malta, Assoc. Prof. Betül Ünlüsü, Assoc. Prof. Nihan Çelebi Ölçüm, Assoc. Prof. Tuğba Davran Candan, Assist. Prof. Levent Organ, Assist. Prof. Semin Funda Oğuz, Assist. Prof. Cem Levent Altan and Assist. Prof. Murat Oluş Özbek for their support, guidance and sincerity.

Last but not least, I would like to dedicate this thesis to my precious parents Vildan-Leon Aruh for their support and encouragement during my whole life. They always believe in me and I am so grateful to have them in my life. Finally, I would like to sincerely thank to Nermin Şen, Nur Çınar, Erhan Saygılı, Berk Gazioğlu, Melek Şekerci Çetin, Binnaz Kavuşturan, Beril Gülkaya and İlayda Acaroğlu Degitz for their moral support during this period.

ABSTRACT

PREPARATION AND CHARACTERIZATION OF POLY (PROPYLENE FUMARATE) (PPF) BASED COMPOSITES AS SCAFFOLDS FOR BONE TISSUE ENGINEERING APPLICATIONS

Poly(propylene fumarate) (PPF) and vinyl phosphonic acid diethyl ester (VPES) based biodegradable and biocompatible polymeric composite systems which were designed to be used as scaffolds for bone tissue defects and tissue regeneration were developed in this study. Intended for this purpose, PPF pre-polymer was synthesized through a polycondensation reaction of propylene glycol and fumaric acid in an excess of propylene glycol. PPF pre-polymer was then cured with the VPES comonomer at body temperature (37°C) with fixed PPF:VPES weight ratio of 70:30, in the presence of benzoyl peroxide initiator, N,N-Dimethyl para-toluidine (DMT) which was utilized as catalyst and varying amounts of Beta-tricalcium phosphate (0-20 wt percent β -TCP) as filler via radical polymerization to prepare biodegradable and biocompatible composite materials that can be used in injectable forms. The structure of the PPF pre-polymer was characterized via FT-IR and $^1\text{H-NMR}$ spectroscopic techniques and molecular weight was determined via gel permeation chromatography (GPC) analysis. Complete cure of the body temperature cured PPF/VPES/ β -TCP composites was confirmed by differential scanning calorimetry (DSC) and thermal degradation profiles were characterized via thermal gravimetric analysis (TGA). Cross-link density was determined via swelling of composites in different solvents. The dispersion of β -TCP particles in the polymer matrix was investigated via scanning electron microscopy (SEM) analysis. Compressive properties were characterized by compression tests. Surface hydrophilicity of the prepared composite materials was analyzed via dynamic contact angle with water measurements. Equilibrium water content of the prepared composites was also determined. Biodegradation rates in PBS buffer solution (pH=7.4) at 37°C were examined via both weight loss and pH measurements for 80 days. All in all, data gathered during entire study implied that the prepared PPF/VPES/ β -TCP composites show significant potential to be used as scaffolds for cartilage tissue engineering applications. This study was supported by TÜBİTAK (114M195).

ÖZET

KEMİK DOKU MÜHENDİSLİĞİ UYGULAMALARI İÇİN POLİ(PROPİLEN FUMARAT) BAZLI KOMPOZİTLERİN YAPI İSKELESİ OLARAK HAZIRLANMASI VE KARAKTERİZASYONU

Bahsi geçen çalışmada, kemik doku mühendisliğinde kullanılması amaçlanan poli (propilen fumarat) (PPF) ve vinil fosfonik asit di-etil esteri (VPES) bazlı biyoyumlu ve biyobozunur polimerik kompozit sistemler geliştirilmiştir. Bu amaç doğrultusunda, PPF pre-polimeri propilen glikol ve fumarik asidin propilen glikol fazlası ortamında polikondenzasyon tepkimesi sonucu sentezlenmiştir. PPF pre-polimeri VPES komonomeriyle sabit bir ağırlık oranında (PPF:VPES=70:30), radikal başlatıcı benzoil peroksit, katalizör N',N'- Dimetil para-toluidin (DMT) ve toplam ağırlığın yüzde 0 ila 20'si aralığında değişen oranlarda beta-trikalsiyum fosfat (β -TCP) dolgu maddesi varlığında vücut sıcaklığında (37 °C) radikal polimerizasyon ile kür edilmiştir. Elde edilen biyoyumlu ve biyobozunur kompozit ürünler enjekte edilebilir formda kullanılabilir. PPF polimerinin yapısı FT-IR ve ¹H-NMR spektroskopik teknikleri ile karakterize edilmiş, moleküler ağırlık jel permeasyon kromatografisi (GPC) ile belirlenmiştir. PPF/VPES/ β -TCP kompozitlerinin oda sıcaklığında kür reaksiyonlarının tamamlandığı diferansiyel taramalı kalorimetri (DSC) analiziyle kanıtlanmış olup, sıcaklığa bağlı bozunma profilleri termal gravimetrik analiz (TGA) yöntemi ile belirlenmiştir. Malzemelerin çözücü içerisinde şişme özelliklerine bağlı olarak çapraz bağ yoğunluğu değerleri hesaplanmıştır. Polimer matriks içerisinde β -TCP parçacıklarının dağılımı taramalı elektron mikroskopi (SEM) ile analiz edilmiştir. Elde edilen kompozit malzemelerin yüzey hidrofilitate analizleri su ile dinamik kontak açısı ölçümleriyle yapılmış olup, kompozitlerin dengedeki su miktarları ayrıca belirlenmiştir. Kompozitlerin *in-vitro* biyobozunma hızları PBS tampon çözeltisi (pH=7,4) içerisinde 80 gün boyunca ağırlık kaybı ve pH değişimi takip edilerek analiz edilmiştir. Sonuç olarak, tüm çalışma boyunca alınan veriler PPF/VPES/ β -TCP kompozitlerinin kemik doku mühendisliği alanında, kırıldak doku iskelesi olarak kullanımının mühim bir potansiyeli olduğunu göstermektedir.

TABLE OF CONTENTS

ACKNOWLEDGEMENTS	iii
ABSTRACT.....	iv
ÖZET	v
LIST OF FIGURES	x
LIST OF TABLES.....	xiii
LIST OF SYMBOLS AND ABBREVIATIONS	xiv
1. INTRODUCTION	1
1.1. DEFINITION AND HISTORY OF BONE TISSUE ENGINEERING	1
1.2. IMPORTANCE OF BONE TISSUE ENGINEERING	1
1.3. POLYMERS USED IN BONE TISSUE ENGINEERING	2
1.4. AIM OF THE STUDY.....	3
2. THEORETICAL BACKGROUND.....	5
2.1. POLYMERS	5
2.1.1. Classification of Polymers.....	6
2.1.1.1. Homopolymers and Copolymers	7
2.1.1.2. Linear, Branched, Cross Linked and Network Polymers.....	8
2.1.1.3. Thermoplastics and Thermosets.....	9
2.1.2. Polymer Synthesis	9
2.1.2.1. Addition (Chain Growth) Polymerization.....	10
2.1.2.2. Condensation (Step Growth) Polymerization.....	10
2.1.3. Amorphous and Crystalline State of Polymers and Mechanical Properties....	11
2.2. BONE TISSUE ENGINEERING	12
2.2.1. Polymeric Scaffolds Utilized in Bone Tissue Engineering	12
2.3. POLY (PROPYLENE FUMARATE) (PPF)	14
2.3.1. Poly(propylene fumarate) and Derivatives of Poly(propylene fumarate)	14

2.3.2. Poly(propylene fumarate) Based Composites	16
3. MATERIALS AND METHODS.....	19
3.1. MATERIALS.....	19
3.2. SYNTHESIS OF POLY(PROPYLENE FUMARATE).....	21
3.2.1. Synthesis of Low Molecular Weight (LMW) PPF.....	22
3.2.2. Purification of the Synthesized PPF.....	23
3.2.3. Synthesis of High Molecular Weight (HMW) PPF.....	24
3.3. CROSS-LINKING OF POLY(PROPYLENE FUMARATE) (PPF) WITH DIETHYL VINYL PHOSPHONATE (VPES) AND PREPARATION OF PPF/VPES/BETA TRICALCIUM PHOSPHATE (β -TCP) COMPOSITES.....	25
3.3.1. Preparation of Thermally Cured PPF/VPES Polymers and PPF/VPES/ β -TCP Composites	25
3.3.2. Preparation of Body Temperature (37 °C) Cured PPF/VPES Polymers and PPF/VPES/ β -TCP Composites.....	26
3.4. STRUCTURAL CHARACTERIZATION OF PPF	27
3.4.1. FT-IR Analysis of PPF.....	27
3.4.2. $^1\text{H-NMR}$ Spectroscopic Analysis of PPF.....	28
3.4.3. Gel-Permeation Chromatography Analysis (GPC).....	28
3.5. CHARACTERIZATION OF PPF/VPES/ β -TCP COMPOSITES.....	29
3.5.1. Cross-link Density Analysis of PPF/VPES Polymer and PPF/VPES/ β -TCP Composites	29
3.5.2. Differential Scanning Calorimetry (DSC) and Thermal Gravimetric Analysis (TGA)	31
3.5.3. Scanning Electron Microcopy (SEM) Analysis	32
3.5.4. Determination of Equilibrium Water Content and Dynamic Contact Angle With Water	33
3.5.4.1. Equilibrium Water Content Analysis.....	33

3.5.4.2. Dynamic Contact Angle With Water.....	34
3.5.5. Mechanical Testing	35
3.5.6. <i>In-vitro</i> Degradation	36
3.5.6.1. pH Measurements.....	37
3.5.6.2. Gravimetric Analysis Method.....	38
4. RESULTS AND DISCUSSION	40
4.1. CHARACTERIZATION OF PPF	40
4.1.1. Structural Analysis of PPF via FT-IR Spectroscopy	40
4.1.2. Structural Analysis of PPF via Proton NMR (¹ H-NMR) Spectroscopy.....	41
4.1.3. Molecular Weight of PPF	44
4.2. CHARACTERIZATION OF PPF/VPES POLYMER AND PPF/VPES/B-TCP COMPOSITES	45
4.2.1. DSC Analysis	46
4.2.2. Cross-link Density Analysis.....	49
4.2.3. Results of TGA.....	51
4.2.4. Results of SEM Analysis.....	53
4.2.5. Equilibrium Water Content (EWC) Analysis.....	54
4.2.6. Contact Angle with Water: Surface Hydrophilicity	56
4.2.7. Compressive Properties	57
4.2.8. Biodegradation Rate (<i>In-vitro</i> degradation)	60
4.2.8.1. Results of Gravimetric Analysis	60
4.2.8.2. Results of pH Measurements	62
5. CONCLUSIONS AND FUTURE WORK	65
5.1. CONCLUSIONS.....	65
5.2. FUTURE WORK.....	67
REFERENCES	68

APPENDIX A.....73



LIST OF FIGURES

Figure 1.1. Schematic representation of cross-linking reaction of PPF with VPES co-monomer.....	4
Figure 2.1. Structure of nitrocellulose	6
Figure 2.2. Classification scheme of polymers	7
Figure 2.3 Schematic representation of homopolymers and copolymers.....	7
Figure 2.4. Linear, branched, cross linked and network structure of polymers	9
Figure 2.5. Schematic representation of chain growth polymerization	10
Figure 2.5. Representation of step growth polymerizations	11
Figure 2.6. Chemical structure of PPF	14
Figure 3.1. PPF synthesis reaction.....	22
Figure 3.2. Apparatus for PPF synthesis.....	23
Figure 3.3. ATI Mattson Genesis Series FT-IR device.	28
Figure 3.4. Carl ZEISS brand EVO 40 model SEM.....	32

Figure 3.5. KSV CAM 101™ Optical contact angle and surface tension measurement device.....	34
Figure 3.6. Instron Universal Dynamic and Fatigue Systems device.....	36
Figure 3.7. Experimental set-up of pH measurement method.....	38
Figure 4.1. FT-IR Spectrum of the synthesized PPF pre-polymer.	41
Figure 4.2. ¹ H-NMR spectrum of LMW PPF.....	42
Figure 4.3. ¹ H-NMR spectrum of HMW PPF.....	43
Figure 4.4. Images of the body temperature cured PPF/VPES polymer and PPF/VPES/β-TCP composites (with 5,10,15,20 wt % β-TCP)	46
Figure 4.5. Image of thermal cured PPF/VPES (70/30)-10% β-TCP composite.	46
Figure 4.6. DSC thermograms of thermally cured PPF/VPES/β-TCP composites (2% BP)	47
Figure 4.7. DSC thermograms of body temperature cured PPF/VPES polymer and PPF/VPES/β-TCP composites (a) first heating cycle (b) second heating cycle.....	48
Figure 4.8. a) Cross-link density and b) molecular weight between cross-links (Mc) values of body temperature (37 °C) cured PPF/VPES polymer and PPF/VPES/β-TCP composites (using 3% BP and 0.3% N, N- DMT).....	50

- Figure 4.9 a) Percent weight vs temperature b) - derivative weight ($-dW/dT$) vs temperature graphs of body temperature cured PPF/VPES polymer and PPF/VPES/ β -TCP composites. 52
- Figure 4.10. SEM images of body temperature cured PPF/VPES/ β -TCP composites with (a) 5% β -TCP (b) 10% β -TCP (c) 15% β -TCP (d) 20% β -TCP at 2000X magnification ... 54
- Figure 4.11. Equilibrium water content values of body temperature cured PPF/VPES polymer and PPF/VPES/ β -TCP composites 55
- Figure 4.12. Contact angle with water for the body temperature cured PPF/VPES polymer and PPF/VPES/ β -TCP composites at 30th second 57
- Figure 4.13. Column graphs of (a) Compressive modulus and (b) Compressive strength of body temperature cured PPF/VPES polymer and PPF/VPES/ β -TCP composites 59
- Figure 4.14. Percent weight loss vs time graphs of body temperature cured PPF/VPES polymer and PPF/VPES/ β -TCP composites 62
- Figure 4.15. pH track of body temperature cured PPF/VPES polymer and PPF/VPES/ β -TCP composites in PBS buffer solution (pH=7.4) at 37 °C..... 64

LIST OF TABLES

Table 3.1. Chemicals used in PPF synthesis and purification.	19
Table 3.2. Chemicals used in preparation of PPF/VPES copolymers an their composites with [Beta]-tricalcium phosphate.....	21
Table 3.2. Amounts of PPF, VPES and BP for preparation of thermal cured composites for a total of 3 gram PPF/VPES material with varying β -TCP content (5,10,15,20 wt %).	26
Table 3.3. Amounts of PPF, VPES, BP and N,N-DMT for preparation of body temperature cured composites for a total of 3 grams PPF/VPES material with varying β -TCP content (5,10,15wt %)	27
Table 4.1. Integral ratios of peak 1 which represents the -CH=CH- protons over peak 4 which represents the methyl (CH ₃) protons of PPF polymer.....	44
Table 4.2. Molecular weight data of the synthesized PPF products as determined via GPC.	45
Table 4.1. Percent weight loss values of body temperature cured PPF/VPES polymer and PPF/VPES/ β -TCP composites at the end of 7 th and 84 th days.....	62

LIST OF SYMBOLS/ABBREVIATIONS

BP	Benzoyl peroxide
DMT	N'-N' – Dimethyl para-toluidine
HAp	Hydroxyapatite
PCL	Poly(caprolactone)
PLGA	Poly(lactic co-glycolic acid)
PLLA	Poly(l-lactic acid)
PPF	Poly(propylene fumarate)
PVPA	Poly(vinylphosphonic acid)
VP	Vinyl pyrrolidone
VPES	Diethyl vinyl phosphonate
β -TCP	Beta tricalcium phosphate

1. INTRODUCTION

Upcoming part of this thesis contains brief and general information about bone tissue engineering, importance of bone tissue engineering, polymers that are utilized in bone tissue engineering applications and the purpose of this study.

1.1. HISTORY OF BONE TISSUE ENGINEERING

Bone tissue engineering aims to produce and develop materials which are designed to be used as scaffolds in bone/tissue defects. There were certain actions taken in the history of bone tissue engineering, which are actually still used and many improvements are also established. First historical sign of tissue engineering was found as the painting of Fra Angelico, which was named as “Healing of Justinian”. Mentioned painting was symbolizing the transplantation of a limb on an injured soldier. In early 1970`s, W.T. Green, M.D, performed many experiments on mice in order to observe bone regeneration. Even though Green`s studies were unsuccessful, he mentioned that it was possible to enhance bone regeneration with correctly prepared biomaterials. After a few years later, Dr. Burke and Dr. Yannas from M.I.T. studied preparation of a skin substitute in order to support the growth of dermal fibroblasts. During mid-1980`s, Dr. Joseph Vacanti and Dr. Robert Langer collaborated to develop a biomaterial in order to accomplish cell delivery, with decreasing unpredictable outcomes. Dr. Vacanti studied intensely not only theoretically, but also experimentally to produce a synthetic biocompatible/biodegradable material. Those studies were seen as a model of a new surgical approach and many tissue engineering studies were started Internationally [1].

1.2. IMPORTANCE OF BONE TISSUE ENGINEERING

Autologous and autonomous bone transplants are very risky and expensive. Both processes may cause permanent injuries not only in receiving side, but also in donor side. Also, surgery may cause deformation, scarring, bleeding, chronic pain and inflammation. In addition, transferring of original bone tissue generally from a cadaver (as known as

allografts) showed many disadvantages like immune system rejections and transmission of infections from one person to another.

At this point, many studies were performed in order to decrease the risk-factor while increasing the quality of life. Recently, preparation and addition of a bone-like material have shown many significant advantages over other applications. In this bone tissue engineering application, a biodegradable/biocompatible material which can easily be accepted by human body with almost no immune system problems is placed in the bone/tissue defect and during recovery placed biomaterial degrades over time while original tissue is formed [2].

1.3. POLYMERS USED IN BONE TISSUE ENGINEERING

Recently, many biodegradable/biocompatible polymeric materials are being used in bone tissue engineering applications (polymer-polymer blends, polymer-ceramic composites, hydrogels etc.). Primarily, poly(lactic-co-glycolic acid)(PLGA) with polyphosphazenes were developed. However, PLGA biomaterials formed acidic products in long-term treatment. Thus, further developments were needed to be made because of the failure of implantation and tissue necrosis [3]. Furthermore, polymeric composites were shown as potential candidates for bone tissue engineering applications. The reason behind this is the natural structure of bone. Bone is originally a composite containing many inorganic hydroxyapatite crystals and organic fibers. Studies showed that polymer-ceramic composites are also successful in bone regeneration. Many composites were prepared using hydroxyapatite with poly(lactic acid) (PLA), PLGA, collagen, gelatin and chitosan [4–6]. Resulting materials have shown enhanced properties when compared with only polymeric materials. Many *in vitro/ in vivo* studies were performed and promising results were obtained for these composite materials.

Poly(propylene fumarate) (PPF), the polymer used in this study is an unsaturated polyester. Its radical copolymerization with a vinyl monomer such as vinyl pyrrolidone results in a biodegradable and biocompatible thermoset. In recent years, many studies on PPF, its copolymers with vinyl pyrrolidone and its composites incorporating inorganic additives

were reported with positive results for their use in bone tissue engineering applications [7–9].

The scaffold material that is going to be used in bone tissue engineering has to have proper mechanical properties, biocompatibility and a tunable biodegradability that must allow bone regeneration as well as osteoconductivity. There are some problems in providing all these properties together for the current biodegradable polymeric materials: such as PLLA, PCL and PPF based systems. In this project the use of VPES comonomer for the crosslinking of PPF pre-polymer is expected to enhance the biocompatibility as compared to the traditional monomers used in the cure of PPF (eg. vinyl pyrrolidone(VP)) [10]. Also, the incorporation of the phosphonic acid ester structure into the PPF network is expected to increase the osteoblast activity as reported in other studies for polyvinyl phosphonic acid (PVPA) based polymers [11,12]. Thus the PPF/VPES copolymer can be classified as a favorable candidate to be utilized as a scaffold material in bone tissue engineering.

In addition, β -tricalcium phosphate (β -TCP) is a proper inorganic additive for the polymeric composite materials designed to be used as scaffolds for bone tissue engineering applications, which improves mechanical properties and enhances osteoconductivity. Calcium phosphates have high affinity for proteins, which enhances cell regeneration [13]. Thus, with the addition of β -tricalcium phosphate (β -TCP) to PPF/VPES copolymers both mechanical properties and osteoconductivity can be improved, in addition the mechanical properties can be tuned with the inorganic filler content of the composites.

1.4. AIM OF THE STUDY

The objective of this study was to prepare and characterize composite materials based on PPF pre-polymer cross-linked for the first time with the VPES comonomer and β -tricalcium phosphate (β -TCP) filler that are designed to be used as scaffolds for bone tissue engineering applications. For this purpose the PPF pre-polymer was first synthesized via the polycondensation reaction of propylene glycol and fumaric acid, the synthesized PPF pre-polymer was then cured with VPES comonomer in the presence of benzoyl peroxide initiator and N',N'-Dimethyl para-toluidine (DMT) catalyst at body temperature (at 37°C) with varying amounts of β -TCP via radical polymerization. After the structural

characterization of the PPF pre-polymer, PPF/VPES copolymer and their β -TCP composites, properties like equilibrium water content, dynamic contact angle with water, thermal degradation profiles, biodegradation profiles and compressive properties were determined and evaluated with respect to β -TCP content of the composites. The cure of the composite formulations applying a high temperature cure cycle (65°C-85°C-100°C) was demonstrated. Thus the composite materials were designed to be used in either injectable or preformed forms as scaffolds for the bone tissue defects.

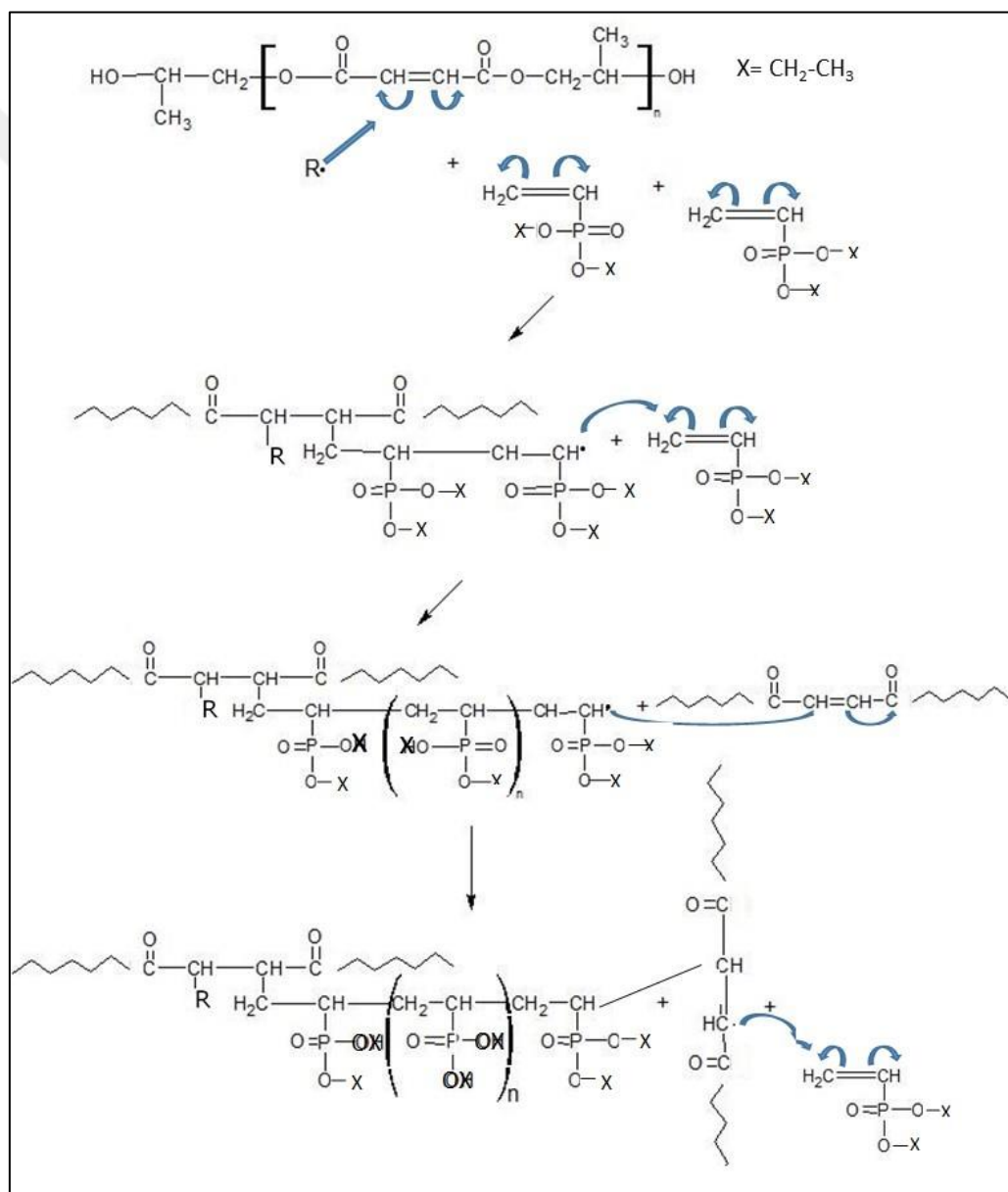


Figure 1.1. Schematic representation of cross-linking reaction of PPF with VPES co-monomer.

2. THEORETICAL BACKGROUND

This section covers the detailed information about polymers, classification of polymers, homopolymers and copolymers. Also, polymer synthesis techniques, bone tissue engineering, polymeric scaffolds that are utilized in bone tissue engineering applications, poly (propylene fumarate) (PPF) and PPF based materials in bone tissue engineering applications are presented in detail.

2.1. POLYMERS

The word 'polymer' was derived by combination of two Latin words, which are 'poly' and 'meres'. Those two Latin words mean 'many parts'. This word was firstly generated by Jons Jacob Berzelius in 1833 and modern definition was made by Hermann Staudinger in 1920. Thus, polymers can be defined as the combination of many repeating units. Repeating units can either be chains or rings, which is also called monomers [14].

Polymers can be investigated in two main categories which are natural polymers (biopolymers) and synthetic polymers. There are many biopolymers such as amber, keratin, collagen, cellulose, wool, starch, DNA etc. Generally biopolymers are responsible for biological functions like energy storage, structural applications, as functional proteins etc. [15].

Although traces of natural polymers can be found even from ancient times, intentional synthesis of a polymer is achieved recently. The first man-made polymer was nitrocellulose (Figure 2.1), which was accomplished by Alexander Parkes in 1862. Mentioned synthesis was done by treating cellulose with a solvent and nitric acid. Furthermore, prepared polymer was treated with camphor and celluloid was produced. Celluloid is highly preferred in film industry, which was used as a replacement of ivory. In addition, Collodion was utilized as surgery dress, which was formed by dissolving nitrocellulose in ether and alcohol [14].

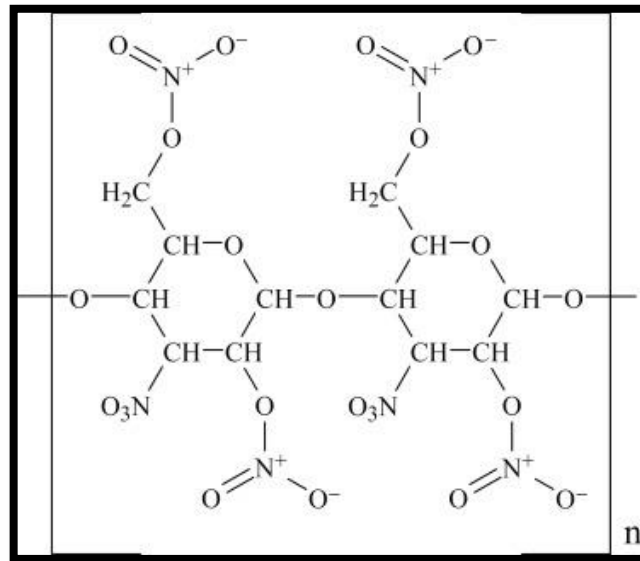


Figure 2.1. Structure of nitrocellulose [16].

On the other hand, synthetic polymers can be produced by chemical reactions. There are many synthetic polymers utilized in daily life such as Nylon, silicone, polyvinyl chloride (PVC), polystyrene etc. Generally these polymers are useful in specific areas such as adhesives, mechanical parts, paint and plastics. In addition, synthetic polymers can be categorized into two, which are thermoplastics and thermosets. These concepts will be given in the upcoming parts of the Theory section [14].

2.1.1. Classification of Polymers

After the foundation of polymers, it was realized that there are many different characteristics of polymers and classification was needed and important. As a result, classifications were done by the behavior of polymers. This is the reason why, there are many types of polymers like thermoplastic polymers (also categorized into two sub-categories), thermoset polymers and elastomers (Figure 2.2). Details of these characteristics will be explained in the following sections [17].

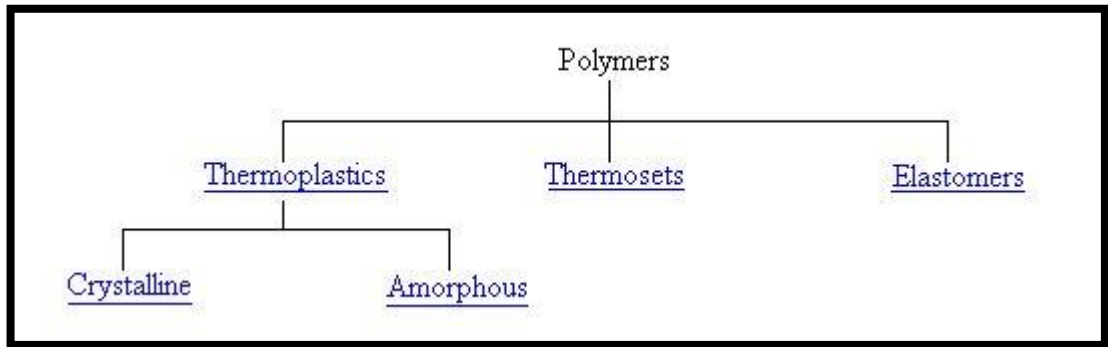


Figure 2.2. Classification scheme of polymers [17].

2.1.1.1. Homopolymers and Copolymers

The chemical structure of a polymer is essential. Generally, chemical structure of polymeric substances can be categorized into two such as homopolymers and copolymers. If there is only one monomer present in the formation of a polymer, the resulting polymer is called a homopolymer. On the other hand, copolymers are formed if the resulting macromolecule is obtained by the reaction of two or more monomers. Although homopolymer structure is a basic polymer structure, copolymer structure may vary due to the polymerization site of the macromolecule. Thus, resulting copolymer may be random copolymer, alternating copolymer, block copolymer and graft copolymer (Figure 2.3) [18].

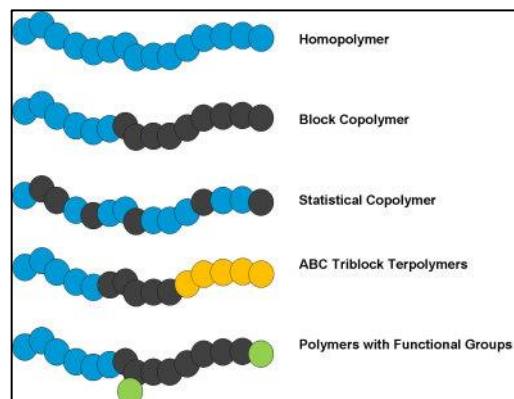


Figure 2.3 Schematic representation of homopolymers and copolymers

2.1.1.2. Linear, Branched, Cross Linked and Network Polymers

As mentioned in theory section 2.1. , polymers are the combination of many repeating units linked together. The term `link` in this case may vary due to participation place of monomers. If monomers in the polymer structure are linked amongst themselves in a straight line, resulting polymeric structure is called as a linear structure. There are many examples to linear polymers such as high density polyethylene, nylon, polyvinyl chloride etc. [18].

Generally, linkage of monomers in polymerization occurs by the linking of two monomers from their active sites. At this point of view, linearity on the resulting macromolecule is unavoidable. However, in common cases, active sides of monomers may prefer to form a bond with another monomer in different angles. This causes branching on the obtained polymeric structure. The examples of branched polymers are starch, low density polyethylene, glycogen etc. [18].

Characteristics of macromolecules vary due to their molecular weight and molecular weight distribution. Also, chain architecture plays a vital role in properties of polymers. When multiple branched macromolecules link together by their branching side and their linear active sides, obtained structure is a cross-linked polymeric structure. Cross-linked polymers show higher mechanical properties. Also, they have slightly better flame resistance and better thermal stability. Cross-linking can be accomplished via radiation or chemical reaction. In addition, reaction of a polymer with a cross-linking agent is called vulcanization [19]. Network structured polymers contain mostly all of the three explained chemical structures.

Physical properties of polymers are also affected by the density of the formed bonds. Density of formed bonds symbolizes the packing of molecules. Thus, when network density increases, rigidity also increases [18]. Linear, branched, cross linked and network structure of polymers is depicted in Figure 2.4.

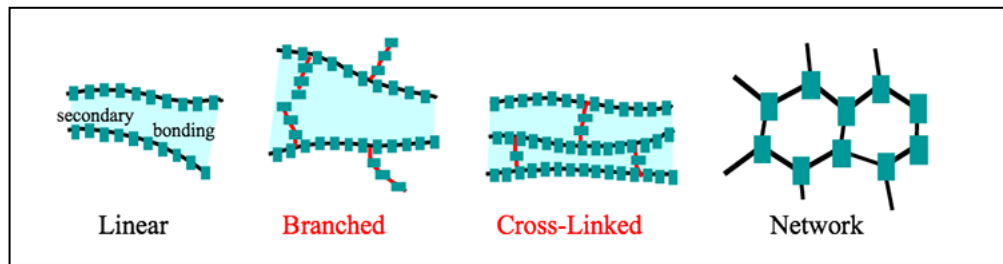


Figure 2.4. Linear, branched, cross linked and network structure of polymers [20].

2.1.1.3. Thermoplastics and Thermosets

As mentioned in the classification of polymers section, macromolecules show different behaviors to temperature change. Thermoplastic polymers can be heated to a viscous liquid-state and cooled back to solid. The reason behind this is the presence of linear and/or branched structures in thermoplastic polymers that do not have an intention to cross-link between each other when heated. Polyethylene, polyvinyl chloride, polystyrene and nylon can be given as examples for thermoplastic polymers [21].

On the other hand, chemical structure of thermoset polymers is altered when heated and many cross-links form amongst themselves. Thus, they are set when heated. Thermoset polymers can be noticed by their highly cross-linked 3D structure and covalent bonds. Thermoset polymers exhibit no melting temperature [21]. Epoxy, melamine formaldehyde, polyester and urea formaldehyde resins can be given as examples of thermosetting polymers.

2.1.2. Polymer Synthesis

It is known that polymers are the results of combination of monomers. Polymer synthesis is the technique that is utilized to link monomers together. Polymers can be synthesized by two main methods, which are addition and condensation polymerization. In late 1920's, Carothers suggested that step-growth and chain polymerization completes the description [15].

2.1.2.1. Addition (Chain Growth) Polymerization

As mentioned in the previous section, polymers are either synthesized via step-growth polymerization or chain growth polymerization. Chain growth polymerization is a relatively fast kinetic scheme where polymerization occurs as a free radical polymerization. In addition, there are three stages in this synthesis technique which are initiation, propagation and termination stages. Schematic representation of chain growth polymerization is shown in Figure 2.5. [22].

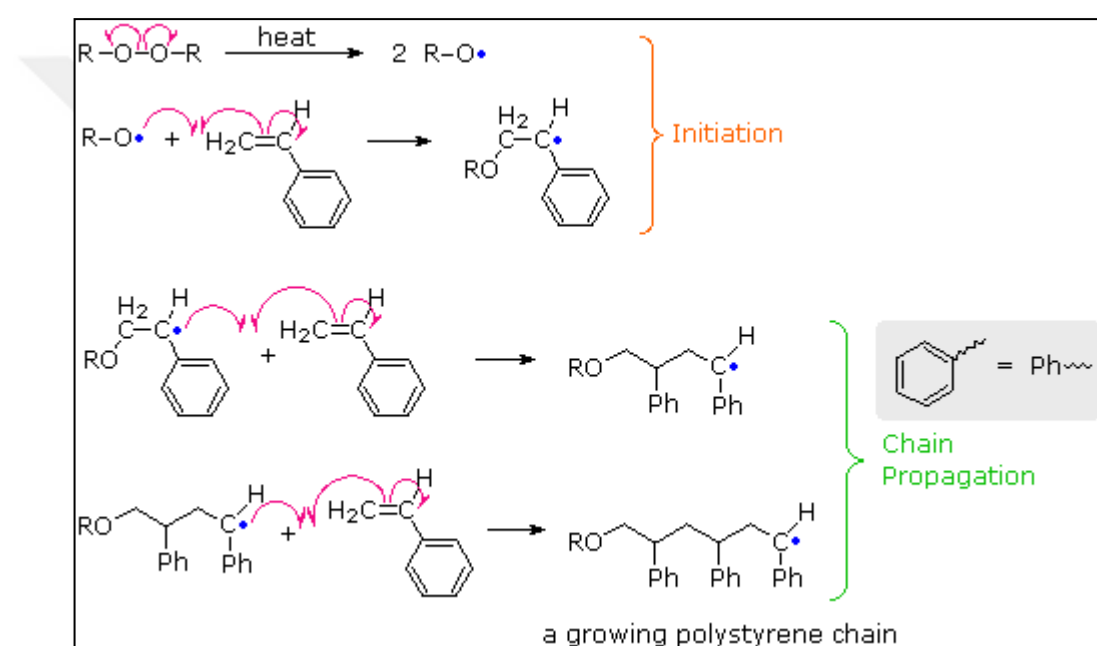


Figure 2.5. Schematic representation of chain growth polymerization[22].

2.1.2.2. Condensation (Step Growth) Polymerization

In step growth polymerization, there is a reaction between bi-functional or multi-functional monomers. That is the reason why, obtained polymers have relatively high molecular weight after several steps. Generally, many natural and synthetic polymers are obtained by step growth polymerization. Due to mechanism of the reaction, it takes more time to complete the reaction in order to obtain high molecular weight polymers. Generally, a small molecule like alcohol, water or acid is produced as a by-product during

polymerization. Step growth polymerization can be symbolized as people holding hands together in a crowded area, as depicted in Figure 2.5. [23].

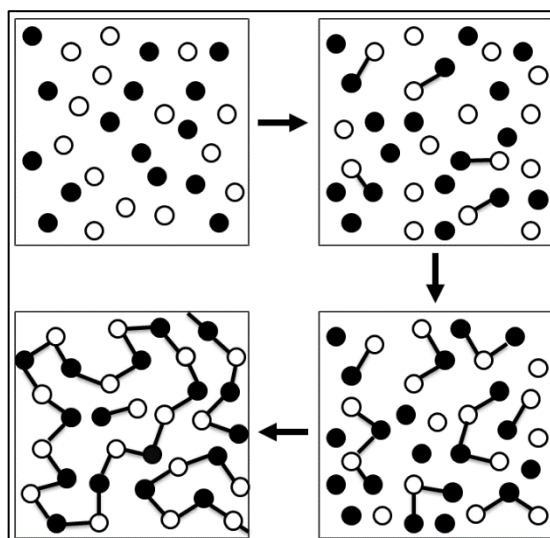


Figure 2.5. Representation of step growth polymerizations [23].

2.1.3. Amorphous and Crystalline State of Polymers and Mechanical Properties

Small molecules can be seen in three different states which are solid, liquid and gas. Polymers have many entangled chains and bonds between molecules that hold them together. Thus, polymers do not have a gas state. In order to understand the states of a polymeric material, crystalline and amorphous states are described. Also, the melt state is an important state to understand the behavior of a macromolecule. Crystalline polymers have high melting point and high rigidity. These polymers are strong, but have low impact resistance. For example, high density polyethylene has high crystallinity (95-99 percent). On the other hand, it is a brittle material. In amorphous polymers, packing of the polymer chains is not regular to form a specific pattern. This is the reason why, they do not have a specific morphology. Amorphous polymers are softer, can be penetrated easily by solvents and they have low melting point.

It is known that crystalline solids are hard, rigid and brittle. Polymers also have a specific temperature (generally low temperatures) where molecular motion is not possible. It is possible to break that polymer in this temperature even though it is a liquid-like macromolecule. However, polymers maintain their molecular disorder. Polymers show a glass-like characteristic in this state. This transition to glass-like state is called 'glass

transition temperature' (T_g). Furthermore, polymers do not have a specific point of melting because of the molecular entanglements and non-crystallinity. However, the very first temperature that melting starts can be observed and recorded. Also, the temperature where the entire polymer becomes liquid can be recorded and the melting point (T_m) range can be obtained. A polymer firstly becomes tacky, and then becomes liquid [24].

2.2. BONE TISSUE ENGINEERING

Bone and tissue regeneration is a process that requires time and patience. Also, patient with a bone/tissue defect faces many challenges during recovery period. Thus, the target of bone tissue engineering applications is to enhance bone regeneration rate and increasing the capability of the patient during recovery.

2.2.1. Polymeric Scaffolds Utilized in Bone Tissue Engineering

In bone tissue engineering, biocompatible and biodegradable polymers are recently being utilized as scaffolds for both structural support and in order to increase cell growth rate. Among these polymers, poly lactic acid (PLLA), poly glycolic acid (PGA) and poly caprolactone (PCL) are the most widely used ones. Many polymeric compositions based on PLLA, PGA and PCL have been patented for being utilized as scaffold in bone tissue engineering and a large number of these studies have been published as well. Most of the related work focused on PLLA, PCL, PGA or the mixture of these polymers such as PLLA-PGA and PLLA-PCL. Poly lactic acid (PLLA), Polyglycolic acid (PGA) and their copolymers, poly(p-dioxanone), trimethylene carbonate and glycolide were utilized in many clinical studies and various publications based on these studies were made [8,25,26] Mentioned studies include majorly biodegradable surgical threads, drug release systems and orthopedic fixation devices such as nails, screws and rods.

In the case of synthetic polymers, utilization of polyesters such as polyglycolide, polylactide, poly caprolactone and poly hydroxybutyrate have been the focus of interest because of ease of degradation due to ester bond hydrolysis and also due to the fact that their degradation products are utilized in metabolic activities and their degradation rate can be controlled by simply varying the structure [27,28].

PGA is a thermoplastic material with high degree of crystallinity and rigidity. Glass transition temperature (T_g) and melting point (T_m) of PGA is 36 °C and 225 °C respectively. It is insoluble in most organic solvents because of its highly crystalline structure. In order to dissolve PGA, solvents with high-fluoride content such as hexa-fluoro isopropanol should be used. It is hard to process PGA containing systems due to its sensitivity to hydrolytic degradation [29]. Thus, process conditions are highly important and require a lot of attention. The main reason of focus on PGA in bone tissue engineering applications is that the degradation product of PGA, glycolic acid is a natural metabolite. PLA on the other hand is a semi-crystalline polymer showing similar hydrolytic degradation rate as PGA. PLA is more hydrophobic than PGA and therefore more durable to hydrolytic attacks. PLA and PGA are amongst the few FDA approved polymers. Generally, their mixtures are prepared with equal ratios of the two polymers. Degradation of these polymers takes place as random hydrolysis between the ester bonds. Many studies indicate that those polymers are biocompatible enough to be used as biomaterials [30,31]. However, some other studies oppose these findings [30,32,33]. Current studies show that utilization of porous structured PLA-PGA scaffolds may cause systemic and/or local reactions or may lead to some side effects during tissue regeneration. Mentioned doubts are increased with the production of toxic solutions during acid degradation of PLA and PGA [33]. This risk increases proportionally with the increasing dimension of the prepared materials. Another mentioned drawback is the release of micro-sized particles during degradation which triggers inflammation [30].

PCL is another widely studied polymer for biomaterial applications. PCL is a semi-crystalline polymer with glass transition temperature (T_g) of -60 °C. It is highly biocompatible and has a low melting point (59-64°C). It is highly preferred in long-term applications due to its slower degradation rate when compared to PLA [30]. PCL has high plasticity and per cent elongation at break however its low mechanical strength limits its use alone, as a bone substitute.

2.3. POLY (PROPYLENE FUMARATE) (PPF)

Poly (propylene fumarate) (PPF) (Figure 2.6) is unsaturated polyester. PPF contains fumarate double bonds which gives a unique chance for being cross-linked either with itself or with another co-monomer like methyl methacrylate [7]. Radical polymerization of PPF with a co-monomer like N-vinyl pyrrolidone (VP) results in a biocompatible and biodegradable thermoset with a network structure. Porosity of these materials can be accomplished by methods like salt leaching. In recent years, many studies have been published on PPF, PPF/VP compositions and their composites with inorganic additives and promising results in terms of their biocompatibility, biodegradability and mechanical properties for their use as bone tissue engineering scaffolds have been reported.

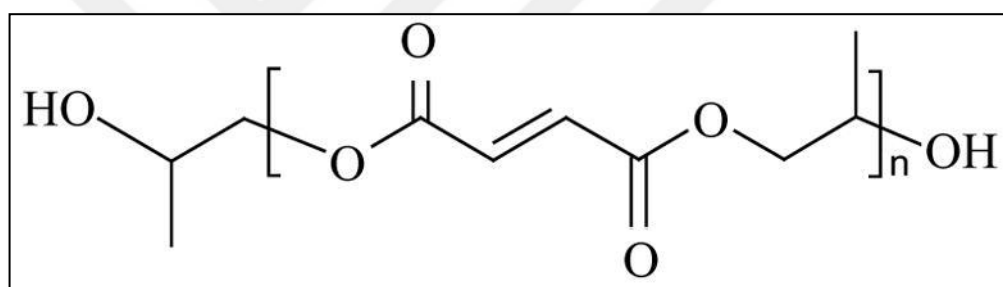


Figure 2.6. Chemical structure of PPF [34]

2.3.1. Poly(propylene fumarate) and Derivatives of Poly(propylene fumarate)

First wide research on PPF was performed by Wang et al. [35] in 2006. This study presented the correlation between molecular weight (chain length) and physical properties of bone tissue engineering scaffold material PPF. As described previously, PPF is an unsaturated polyester with reactive fumarate double bonds thus it can form a cross-linked (network) structure via radical polymerization with itself or other co-monomers such as methyl methacrylate or N-vinyl pyrrolidone [7]. These characteristics indicated PPF as a promising biopolymer for tissue engineering applications. Generally studies on PPF involved the cure of PPF with low molecular weight poly acrylate, methacrylate or fumarate resins with or without VP and the investigation of properties like the cure conditions, mechanical properties and biodegradation rates. In addition various studies

focused on the preparation and characterization of composites based on PPF, its derivatives and inorganic additives such as hydroxyapatite and calcium phosphates.

In one representative study, biodegradable network polymers were prepared via cure of PPF with the cross-linking agent PPF-diacrylate using both thermal and photo-initiation systems [8]. Benzoyl peroxide was used as a thermal initiator with N, N dimethyl p-toluidine as a catalyst and bis (2, 4, 6-trimethylbenzoyl) phenylphosphine oxide (BAPO) was used as the photo-initiator. Statistical results indicated that both thermal cross-linking and photo-cross linking have significant positive effects on mechanical properties. In addition it was also reported that for the same double bond ratios, both compressive modulus and strength values were higher for the PPF/PPF- diacrylate systems cured with BAPO via photo initiation. However, a significant difference in the yield of polymerization was not observed between the thermal and photo initiated systems.

In another related study by Wang et al., PPF was photo-cross linked with poly caprolactone fumarate (PCLF) with varying PPF/ PCLF ratios and mechanical properties, surface morphology and in-vitro cell interaction of these polymers were investigated [35]. Results of this study indicated that, mechanical properties (compressive modulus, strength, surface hardness) and biocompatibility of PPF/PCLF network polymers improved with increasing amounts of PPF and that these materials did not show cytotoxicity and therefore were suitable to be used for bone tissue engineering. In another study, He et al., [7] worked on injectable and biodegradable composites based on PPF that can be *in-situ* cured with polyethylene glycol-dimethacrylate (PEG-DMA) and beta-tri-calcium phosphate (β -TCP). The results of this study showed that utilization of β -TCP on PPF and polyethylene glycol-dimethacrylate (PEG-DMA) based materials improve mechanical properties such as compressive modulus, compressive strength and hydrophilicity of the resulting biomaterials. Likewise, a study of Mitha et al. reported that a resin containing a mixture of PPF with a hydroxyl ending poly (castor oil fumarate) (PCF) as the cross-linker components, N-vinyl Pyrrolidone as the comonomer and hydroxyapatite as the inorganic filler, could be utilized as an injectable in-situ cross-linking polyester. In this formulation, a radical initiator such as benzoyl peroxide and a catalyst such as N,N dimethyl aniline was utilized [36]. Also, mechanical properties and cross-link density of resulting materials increased with increasing VP content. Resulting composites had a hydrophilic character

and they were reported as compatible with L929 fibroblast cells. Obtained data points the fact that PPF/NVP/ β -TCP composites can be a perfect replacement for trabecular bone.

In a similar study, authors reported the biocompatibility of PPF cross-linked with polyethylene glycol-diacrylate (PEG-DMA) and beta-tricalcium phosphate (β -TCP) based composites. The composites were designed to be utilized as in-situ cross-linking, injectable and biodegradable material.

Lewandorowski et al. [9] investigated the effect of foaming poly(propylene fumarate) cements on bone defects in regeneration stage. Foaming was accomplished by addition of bicarbonate to the medium. This way, resulting biomaterials did not only have a porous structure, but also the utilized foaming agent was a product in metabolic activity. In other words, the resulting porous material was harmless. Trials were done on the tibia bone of rabbits and both groups had no infection. Histological and histomorphometric analysis indicated that, after first week regeneration was observed on the trial group. However, there was no regeneration on the control group. This study proved that PPF cement foamed with bicarbonate was a porous, biodegradable and biocompatible material which promoted bone regeneration. Thus, this material was found suitable to be used as a scaffold in Tibia bone defects.

2.3.2. Poly(propylene fumarate) Based Composites

It is always important to obtain a material with suitable characteristics for a specific application. Recently, many studies and commercial products prove that materials with multi-components show different types of advantages in terms of properties to different situations as compared to each component alone. Materials that contain two or more types of components are called 'composite materials'. Composite materials are mostly preferred because they are the combinations of multiple useful components.

A great number of studies concentrated on composites based on PPF and inorganic fillers such as hydroxyapatite and phosphates for their use as scaffolds for bone tissue engineering. In a relatively recent study, the aim was to prepare PPF based composites by mixing di-calcium phosphate dihydrate (DCPD) with PPF [37]. Calcium phosphate fillers have the ability to improve properties such as osteoconductivity and absorption when used

as a bone scaffold. However, due to their fragile mechanical characteristics, their composites with a polymer such as PPF are highly preferred. In the mentioned study, 3-Dimensional and macro porous materials were prepared with rapid prototyping technique. After characterization, the prepared PPF-DPCD materials were implanted to a rabbit's calvarial defects. According to the *in-vivo* studies, there was not any significant enhancement in recovery rate. However, bone has the ability to regenerate itself through the pores of PPF-DPCD material thus this composite material was reported as a promising scaffold material for bone tissue engineering applications. In another study by Kee-woon-Lee[35], a series of nano composites of PPF reinforced with varying ratios of hydroxyapatite (HAp) were prepared. Addition of HAp on to cross-linked PPF did not enhance the mechanical properties further because the highly cross-linked PPF already exhibited high modulus. On the other hand, hydrophobicity, cell attachment rate, cell dispersion rate and cell proliferation improved significantly with HAp addition. The results of the study indicated that PPF/HAp based materials were suitable as hard bone tissue replacements because of excellent mechanical properties and osteoconductivity. In another study carried on PPF//HAp based composites, Jaybalan et al. investigated the effect of radiation process on biodegradation and mechanical properties of the composites. It was reported that the application of 3Mrad dosage of radiation to these formulations improved the degree of cross-linking and mechanical strength.

The study of Peter et al. was also a great investigation about the cross-linking characteristics of injectable PPF based composite bone cements. In this study, PPF, N-vinyl pyrrolidone (N-VP), benzoyl peroxide (BP), NaCl and beta-tricalcium phosphate (β -TCP) were used as the bone cement. NaCl was leached after composite preparation. Effects of molecular weight of PPF, N-VP/PPF and BP/PPF ratios and NaCl weight percentage on the cross-linking temperature and compressive modulus and strength were investigated. Cross-linking temperatures were relatively close to each other for all formulations (38-48°C) which were dramatically lower than poly (methyl methacrylate) PMMA cements (98°C). The mechanical properties of the injectable PPF/ β -TCP materials indicated that these materials were suitable as scaffolds in trabecular bone replacements however the effect of the composites on bone tissue regeneration was not investigated. The molecular weight of PPF did not have a significant effect on mechanical properties.

PPF based composites are not only used as scaffolds, but also they can be used as drug release agents. In a study by Kempen et al. [3], for the controlled release of bioactive molecules, PPF and PLGA microspheres were prepared and these microspheres were placed into injectable porous PPF structural scaffolds. The porous composite structure was accomplished with gas bubbles technique. The developed scaffolds exhibited a network inter-porous structure. Reported results indicated that prepared scaffolds were able to release a model drug successfully for 28 days.

In another study by Wu et al [38], a new injectable and biodegradable composite based on PPF, N-VP and biphasic alpha tricalcium phosphate/hydroxyapatite(HAp) has been prepared and in vitro characteristics of these composite materials were determined. The results of this study indicated lower cure temperatures as compared to PMMA and neat PPF/HAp cements, adequate initial compressive strength and a stepwise degradation for these bone cements.

There are several more studies based on PPF matrix and its composites in literature, however only the ones that are related to the topic of this study were presented in this section.

3. MATERIALS AND METHODS

3.1. MATERIALS

This section gives information about the chemicals used in the synthesis and purification of PPF which are listed in Table 3.1. Also, those that are used in the preparation of PPF/VPES copolymers and their composites with [Beta]-tricalcium phosphate are presented in Table 3.2.

Table 3.1. Chemicals used in PPF synthesis and purification.

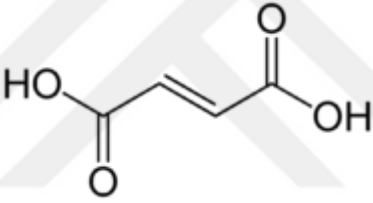
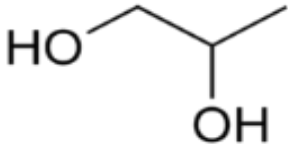
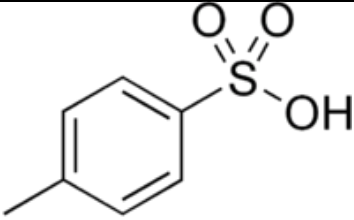

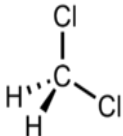
Chemical Name	Formula	Molecular Structure	Provider
Fumaric Acid	$C_4H_4O_4$		Alfa Aesar
Propylene Glycol	$C_3H_8O_2$		ChemCruz™ Santa Cruz Biotechnology. INC.
P-Toluene Sulphonic acid	$C_7H_8O_3S$		Fluka
Hydroquinone	$C_6H_6O_2$		Sigma-Aldrich
Dichloromethane puriss	CH_2Cl_2		Sigma-Aldrich

Table 3.1 Cont'd


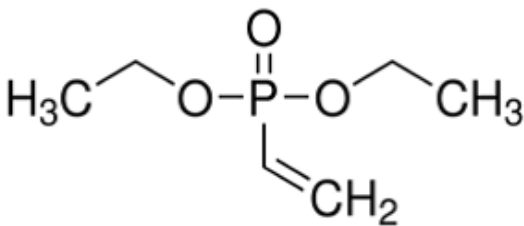
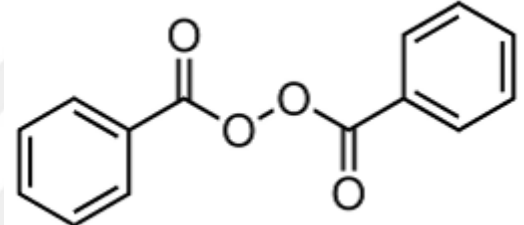
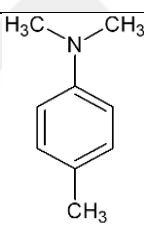
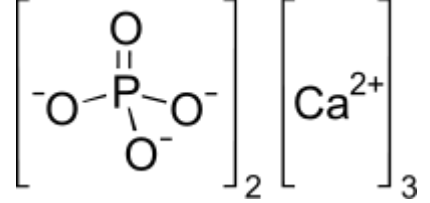
Methanol	CH ₃ OH	$\begin{array}{c} \text{H} \\ \\ \text{H}-\text{C}-\text{OH} \\ \\ \text{H} \end{array}$	Merck Millipore
Calcium Chloride Anhydrous. granular	CaCl ₂	$\text{Cl}-\text{Ca}-\text{Cl}$	Sigma-Aldrich
Diethyl Ether	C ₄ H ₁₀ O		Sigma-Aldrich

Table 3.2. Chemicals used in preparation of PPF/VPES copolymers and their composites with [Beta]-tricalcium phosphate.

Chemical Name	Formula	Molecular Structure	Provider
Diethyl vinyl phosphonate (VPES)	$C_6H_{13}O_3P$		Sigma-Aldrich
Benzoyl Peroxide (BP)	$C_{14}H_{10}O_4$		Merck
N,N-dimethyl-p-toluidine	$C_9H_{13}N$		Alfa Aesar
[Beta]-tricalcium phosphate	$Ca_3(PO_4)_2$		Fisher Scientific

3.2. SYNTHESIS OF POLY(PROPYLENE FUMARATE)

Poly (propylene fumarate) (PPF) was synthesized from propylene glycol and fumaric acid using hydroquinone as a radical inhibitor and p-toluene sulfonic acid as the catalyst. The synthesis reaction is shown in Figure 3.1.

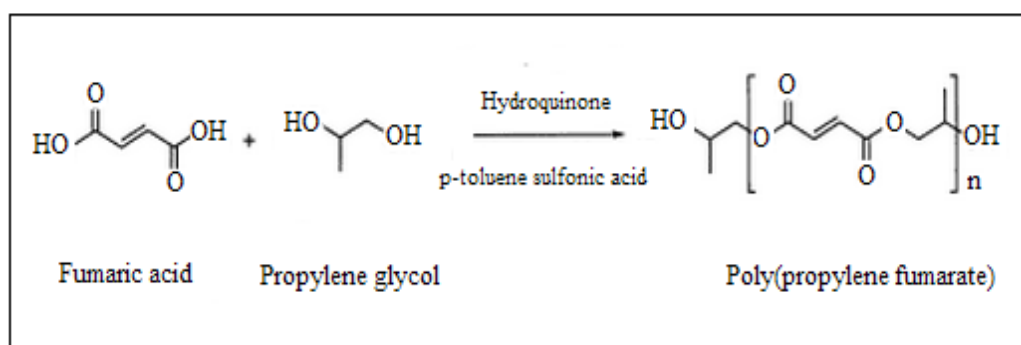


Figure 3.1. PPF synthesis reaction

Poly(propylene fumarate) (PPF) was synthesized in laboratory by reacting propylene glycol and fumaric acid with a stoichiometric ratio of 1.65 : 1.5 moles. P-toluene sulphonic acid was used as the catalyst and its weight was 0.4wt percent of the total weight of propylene glycol and fumaric acid. 0.1wt percent hydroquinone was utilized as the radical inhibitor. To prevent gelation. During this study, molecular weight of synthesized PPF was adjusted by varying the reaction time and addition of excess propylene glycol over time. The differences of two procedures will be explained below.

3.2.1. Synthesis of Low Molecular Weight (LMW) PPF

The procedure for the LMW PPF synthesis is described with the following steps:

- i. 125.5 gram of propylene glycol and 174.1 gram of fumaric acid were put into a 500ml round bottom flask equipped with a mechanical stirrer, a thermocouple, a nitrogen gas inlet and a Dean stark apparatus connected to a condenser. The apparatus for the reaction is shown in Figure 3.2.
- ii. 1.203 gram of p-toluene sulfonic acid and 0.290 gram of hydroquinone were added to the mixture in the flask.
- iii. The contents of the flask were heated to 145°C using a heating mantle. The solution was stirred at this temperature for 3 hours at 100-150 rpm.
- iv. At the end of heating for 3 hours at 145°C, the temperature of the reaction medium was increased to 180°C and the solution was stirred at this temperature for 1 hour.
- v. Approximately 30 mL of water was collected as the byproduct of the reaction.

- vi. At the end of 1 hour at 180°C, the solution was left to cool to room temperature to prevent further polymerization.

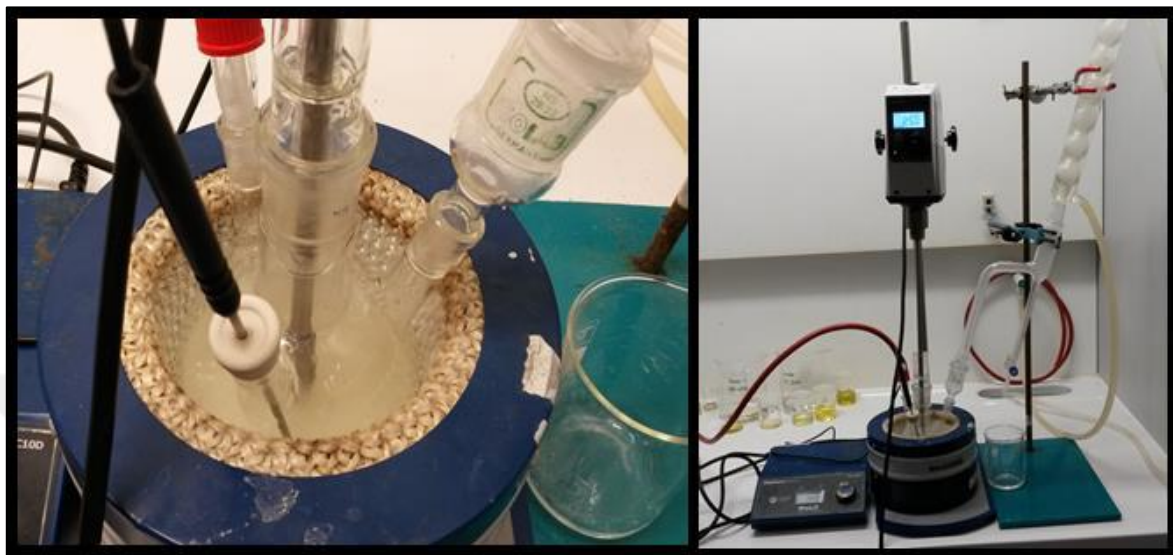


Figure 3.2. Apparatus for PPF synthesis

3.2.2. Purification of the Synthesized PPF

The purification steps are outlined below.

- i. Synthesized poly (propylene fumarate) was heated in an oven to around 130°C to reduce its viscosity and the crude PPF product was transferred to an erlenmeyer flask.
- ii. The crude PPF product was dissolved in 150 ml of dichloromethane (CH_2Cl_2).
- iii. Vacuum filtration was performed in order to eliminate the catalyst and the unreacted fumaric acid.
- iv. After vacuum filtration, 100 ml of 20:80 ratio of methanol-water solution was prepared and the PPF solution was washed with the methanol-water solution. Two phases occurred after the addition of methanol-water solution. There was 80 ml of water with unreacted propylene glycol at the top phase. PPF in dichloromethane was at the bottom phase. The PPF solution was taken and the top water phase was discarded.

- v. Calcium chloride (CaCl_2) was added to PPF solution in order to eliminate residual water; CaCl_2 was added until the solution became totally clear.
- vi. Vacuum filtration was performed in order to remove CaCl_2 particles.
- vii. Finally, 150 ml of diethyl ether was added to the PPF solution in dichloromethane and the PPF in the diethyl ether phase was taken and put in the rotary evaporator to evaporate the added diethyl ether. The obtained PPF product was a yellow colored, transparent viscous resin at room temperature.

3.2.3. Synthesis of High Molecular Weight (HMW) PPF

The procedure for the HMW PPF synthesis is described with the following steps:

- i. 110.5 gram of propylene glycol and 174.1 gram of fumaric acid were put into a 500ml round bottom flask equipped with a mechanical stirrer, thermocouple, nitrogen inlet and a Dean stark apparatus connected to a condenser. The apparatus for the reaction is shown in Figure 2.2.
- ii. 1.203 gram of p-toluene sulfonic acid and 0.58 gram of hydroquinone (0.2wt percent) were added to the mixture in the flask.
- iii. The contents of the flask were heated to 145°C using a heating mantle. The solution was stirred at this temperature for 8 hours at 100-150 rpm.
- iv. At the end of heating for 8 hours at 145°C , the temperature of the reaction medium was increased to 180°C and the excess propylene glycol was added as 0.05 mole fractions at the end of 1 hour intervals. So, the reaction solution was stirred at 180°C for a total of 5 hours.
- v. At the end of 5 hours at 180°C , the solution was left to cool to room temperature in order to prevent further polymerization.
- vi. Purification procedure of the synthesized HMW PPF was the same with the LMW PPF purification procedure.

3.3. CROSS-LINKING OF POLY(PROPYLENE FUMARATE) (PPF) WITH DIETHYL VINYL PHOSPHONATE (VPES) AND PREPARATION OF PPF/VPES/BETA TRICALCIUM PHOSPHATE (β -TCP) COMPOSITES

3.3.1. Preparation of Thermally Cured PPF/VPES Polymers and PPF/VPES/ β -TCP Composites

- i. Firstly, pre-synthesized LMW PPF was heated on a heater. The viscosity of polymer was decreased by heating and it was heated to approximately 50 °C.
- ii. For weighing the ingredients of the mixtures, a magnetic fish was put into a glass vial that was placed on laboratory scale and for the accurate weighing it was tared. According to desired ratios, the components of the mixtures were weighed. Amounts of the components of thermal cured composites for a total of 3 grams of PPF/VPES material with varying β -TCP content are listed in Table 3.2.
- iii. Weighing process must be performed quickly. In order to mix them, magnetic stirrer was used and a homogeneous mixture was obtained. Further heating must not be done at this step as it may start the curing process.
- iv. The prepared homogeneous mixture was poured into glass vials
- v. The vials were closed and they were put into a pre-heated oven and heated for first 2 hours at 65°C, then for 2 hours at 85 °C and then for 5 hours at 100°C.
- vi. After cooling to room temperature, all samples were removed from the vials.

Table 3.2. Amounts of PPF, VPES and BP for preparation of thermal cured composites for a total of 3 gram PPF/VPES material with varying β -TCP content (4,6,8,10,12,15 wt percent)

	Weight Percentage (%)	Weight(g)
PPF	70	2.1
VPES	30	0.9
BP	2	0.06

3.3.2. Preparation of Body Temperature (37 °C) Cured PPF/VPES Polymers and PPF/VPES/ β -TCP Composites

- i. Firstly, pre-synthesized HMW PPF was heated on a heater. The viscosity of polymer was decreased by heating and it was heated to approximately to 50 °C.
 - ii. HMW PPF was put into a glass vial with a magnetic stirrer while the temperature was kept constant.
- Afterwards the ingredients of the composite formulations were added in the following order. The amounts of the components of composite formulations for a total of 3 grams of PPF/VPES material with varying β -TCP content are listed in Table 3.3.
- iii. Specified amount of VPES co-monomer was put onto PPF polymer and mixing was performed isothermally.
 - iv. Specified amount of benzoyl peroxide was added into the mixture and mixing was continued.
 - v. Specified amount of β -TCP was put into the mixture and mixing was continued.
 - vi. The catalyst (N, N-DMT) was added by using a micro pipette and mixing was continued.
 - vii. Weighing process must be performed quickly. In order to mix the components of the formulation, magnetic stirrer was used till a homogeneous mixture was obtained. Temperature was kept constant during mixing.
 - viii. The prepared homogeneous mixture was poured into glass vials under Nitrogen atmosphere.

ix. The vials were closed and they were put into a pre-heated oven at 37 °C.

All samples were removed from the vials at the end of approximately 2 hours at 37 °C, after the curing process was complete.

Table 3.3. Amounts of PPF, VPES, BP and N,N-DMT for preparation of body temperature cured composites for a total of 3 grams PPF/VPES material with varying β -TCP content (5,10,15wt percent)

	Weight Percentage (%)	Weight(g)
PPF	70	2.1
VPES	30	0.9
BP	3	0.09
N,N-DMT	0.3	0.009

3.4. STRUCTURAL CHARACTERIZATION OF PPF

3.4.1. FT-IR Analysis of PPF

In this work, FT-IR spectroscopy was mainly used to characterize the structure of the synthesized PPF pre-polymer with the assignment of characteristic peaks. All samples were run on an ATI Mattson Genesis Series FT-IR spectrometer (Figure 3.3). For the FT-IR analysis of the PPF pre-polymers, firstly samples were placed in KBr and pellets were pressed at 5000-10000 psi. After a background scan of the pure KBr pallet was taken, each sample was scanned 16 times with a resolution of 4 cm^{-1} in the 400-4000 cm^{-1} region.

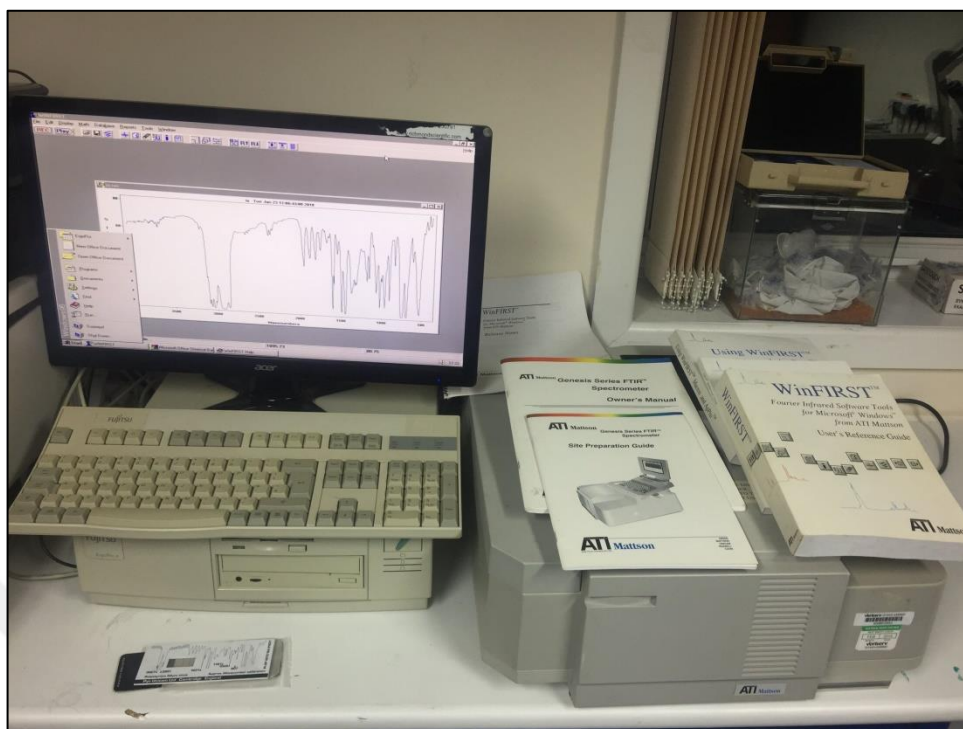


Figure 3.3. ATI Mattson Genesis Series FT-IR device.

3.4.2. $^1\text{H-NMR}$ Spectroscopic Analysis of PPF

$^1\text{H-NMR}$ spectroscopy was used to characterize the synthesized poly (propylene fumarate) (PPF). Samples were prepared for NMR analysis by dissolving 0.1 g of PPF in 1 ml deuterated chloroform (CDCl_3). A Bruker AM250 with a magnetic field strength of 250MHz was used as the NMR spectrometer. A spectral window of 2000Hz. and a pulse width of 90° were used and the digital resolution was 0.427 Hz/pt. Samples were at 293K during the measurement.

3.4.3. Gel-Permeation Chromatography Analysis (GPC)

In order to determine the molecular weight of the prepared PPF polymers, GPC analysis was used. Tetrahydrofuran (THF) was used as the solvent. Model of the device was Agilent 1100 Series and flowrate was set to 0.5 mL/min. The utilized device was equipped with a refractive index detector. 2 mg of PPF sample was dissolved in 1mL THF and

filtered by a Teflon filter with a pore size of 0.45 μm and then injected into the column (PL-gel 5 μm , Mixed D). Analysis was performed at room temperature (25°C) and linear polystyrene standards ($M_p = 500\text{-}300.000\text{ g/mol}$) were used for calibration.

3.5. CHARACTERIZATION OF PPF/VPES/ β -TCP COMPOSITES

For the characterization of prepared PPF/VPES/ β -TCP composite materials, various analyses were performed such as cross-link density analysis, differential scanning calorimetry (DSC), thermal gravimetric analysis (TGA), scanning electron microscopy (SEM), determination of equilibrium water content and dynamic contact angle with water, mechanical testing and analysis of *in-vitro* degradation (via pH and weight loss analysis).

3.5.1. Cross-link Density Analysis of PPF/VPES Polymer and PPF/VPES/ β -TCP Composites

Cross-linking of the polymer chain is highly substantial for controlling the characteristics of many properties of polymeric materials. Increase in the cross-link density, increases the rigidity of the amorphous polymers which causes to have higher softening temperatures and higher modulus values. Furthermore, increase in cross-link density decreases the elongation at break and swelling and also increases the glass transition temperature (T_g) of the polymeric materials.

In this study, cross-link density of the prepared materials was determined by swelling tests. Cured materials were put into different solvents (dimethyl acetamide, dimethyl formamide, toluene, tetrahydrofuran and water) for two days. Swelling characteristics of the prepared polymeric materials were investigated [39].

Solubility parameter of polymer (δ_p) was taken as the solubility parameter for the solvent (δ_s) which caused maximum swelling which was found as THF. Firstly, swelling coefficient of the cured material inside THF was calculated by Equation 2.1 [40];

$$Q = \frac{\text{Weight of the solvent in Swollen polymer}}{\text{Weight of Swollen polymer}} \times \frac{\text{Density of Polymer}}{\text{Density of Solvent}} \quad (3.1)$$

Volume fraction of the swollen polymer (V_r) was calculated by the utilization of swelling coefficient. Percentage of effective cross-links in swollen polymer (γ) was determined by the help of modified Flory-Rehner Equation [36]. Thus, cross – link density can be calculated by using Equation 2.2.

$$\gamma = \frac{-[V_r + \chi V_r^2 + \ln(1 - V_r^2)]}{d_r V_0 \left(V_r^{\frac{1}{3}} - \frac{V_r}{2} \right)} \quad \left(\frac{\text{mol}}{\text{cm}^3} \right) \quad (3.2)$$

Molecular weight between cross-links (\overline{M}_c) and volume fraction of the polymer (V_r) was calculated by using Equation (2.3) and Equation (2.4);

$$\overline{M}_c = \frac{1}{\gamma} \quad (3.3)$$

$$V_r = \frac{1}{1 + \theta} \quad (3.4)$$

Polymer-lattice interaction parameter (χ) was taken as 0.34 where the solubility parameter of polymer was equal to solubility parameter of the solvent and the molar fraction of the solvent was taken into account as V_0 .

3.5.2. Differential Scanning Calorimetry (DSC) and Thermal Gravimetric Analysis (TGA)

DSC analysis was performed on both thermally and body temperature cured PPF/VPES/ β -TCP samples to see whether the cure reactions of these samples were complete or not. The DSC measurements were performed on a Perkin Elmer Differential Scanning Calorimeter in nitrogen atmosphere. At most 10 mg of the cured PPF/VPES polymer or its composite was put into an aluminum pan and covered with caps, an empty aluminum pan was also prepared to be used as the reference. The two aluminum pans were then placed into the chamber. Then, they were scanned from 20°C to 250°C at a heating rate of 10°C/min. In order to observe post-cure exotherms, heating cycle was performed twice for body temperature cured PPF/VPES and PPF/VPES/ β -TCP composites. After the measurement, collected data was used to construct heat flow vs temperature plots. The procedure for the DSC analysis of the samples is outlined below.

- i. Nitrogen tank was turned on and adjusted to an average pressure of 50 psi.
- ii. Up to 10 mg of sample was cut off with a tweezer and weighed. This piece was placed in a 120 ml aluminum pan. Pan was closed with the lid. The press was used to crimp the lid for the sample pan.
- iii. Pan which includes the sample was placed on the back stand of the oven and blank pan was placed in the front of stand of the oven. Then oven was closed.
- iv. Ramps and isotherms were set like below:

Ramp ₁ :	T ₁ =20 °C	T ₂ =300 °C	Heating rate =10 °C/min
Isotherm:	T ₁ =300 °C	time=5 min	
Ramp ₂ :	T ₁ =300 °C	T ₂ =20 °C	Heating rate = 99 °C/min
Isotherm:	T ₁ =20 °C	time=5 min	
- v. Analysis was started. Analyses were carried out under nitrogen atmosphere.
- vi. Heat flow vs. temperature data was obtained from the analysis.
- vii. Heat flows vs. temperature plots were constructed.

The thermal degradation behavior of the PPF/VPES copolymer and its β -TCP composites was analyzed using a Perkin Elmer – Pyris 1 TGA analyzer. For each analysis, a 5 – 7 mg of sample was heated from 25°C to 800°C at 10°C/min heating rate, in an oven in nitrogen

atmosphere (20 mL/min). Weight loss was observed with increasing temperature. Percent weight loss versus temperature plots were constructed and analyzed for all of the samples tested.

3.5.3. Scanning Electron Microcopy (SEM) Analysis

The fracture surface morphologies of body temperature cured PPF/VPES/ β -TCP composites with varying β -TCP ratios were characterized by the SEM analysis. For this purpose, samples were frozen in liquid nitrogen and then broken with a single move. SEM images were taken at high vacuum by application of 10 kw of voltage with a Carl ZEISS brand EVO 40 model SEM (Figure 3.4) after these fracture surfaces were coated with gold dust (~ 5 nm thickness) by the Baltec brand SCD 005 Sputter Coater model gold coating device for 15 seconds.

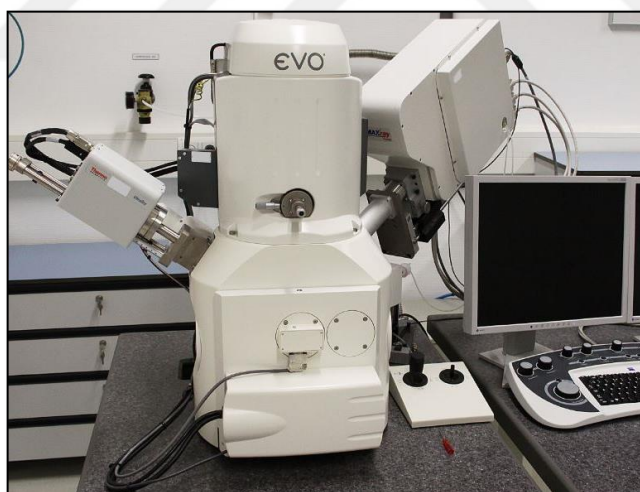


Figure 3.4. Carl ZEISS brand EVO 40 model SEM

3.5.4. Determination of Equilibrium Water Content and Dynamic Contact Angle With Water

3.5.4.1. Equilibrium Water Content Analysis

Equilibrium water content (EWC) of body temperature cured PPF/VPES polymer and PPF/VPES/ β -TCP composites was determined gravimetrically and the values were evaluated with regard to composition of the samples. In order to perform equilibrium water content test, samples were washed with dichloromethane to get rid of any unreacted PPF and VPES and after drying initial weight of the samples were recorded. 1 X Phosphate buffer solution (PBS) was introduced with distilled deionized water inside the sample tubes and the final weight of the samples were obtained at the end of 36 hours. Following procedure was carried out;

- i. Each sample was washed with dichloromethane.
- ii. Washed samples were dried in open air for 24 hours and all samples were put into vacuum oven at 40 °C for 6 hours.
- iii. Dried samples were taken out of vacuum oven and weighed as W_1
- iv. 1X PBS buffer solution was added to each glass bottle and a known mass of the sample was placed in the bottle and allowed to swell to equilibrium.
- v. Weight of the samples was monitored periodically for 36 hours at room temperature.
- vi. At the end of 36 hours, final weight of each sample was recorded as W_2 after the removal of any water on the surface of the sample. From the difference in weights, equilibrium water content was calculated by Equation 2.5. Tests were performed in duplicate for each composition.

$$\text{Equilibrium water content} = \left[\frac{W_2 - W_1}{W_2} \right] \times 100 \quad (3.5)$$

3.5.4.2. *Dynamic Contact Angle with Water*

In order to determine the dynamic contact angle with water for the body temperature cured PPF/VPES polymer and PPF/VPES/ β -TCP composites, disc shaped samples were prepared. All of the samples were polished in order to eliminate the surface difference of the samples. Therefore, the obtained data from the analysis would only depend on the hydrophilicity of the surface of each prepared material. Hamilton syringe was utilized in order to stabilize the volume of the distilled water and KSV CAM 101TM Optical contact angle and surface tension measurement device (Figure 3.5) was used during analysis. Water with specified volume was dropped onto the surface of the sample and first image was taken at 30th second. Other images were taken with ten second intervals with a total of 15 images. After the analysis, average contact angle was calculated and average contact angle at 30th second was analyzed for comparison of samples.

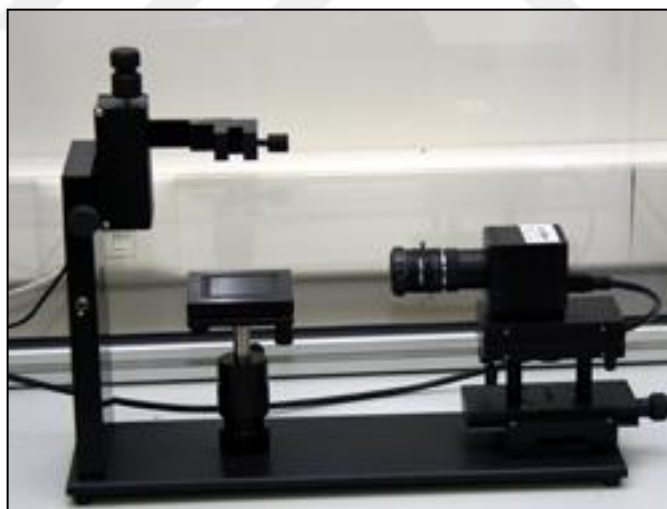


Figure 3.5. KSV CAM 101TM Optical contact angle and surface tension measurement device

3.5.5. Mechanical Testing

Compression test was applied on disc shaped PPF/VPES polymer and PPF/VPES/ β -TCP composite samples. During analysis, Instron Universal Dynamic and Fatigue Systems device (Figure 3.6) was utilized. Samples were placed inside the device and the force ramp rate was adjusted to 0.1 N/min with a compression rate of 1 mm/min. According to the results obtained from this device, stress (MPa) vs strain (percent) graphs were plotted and compressive modulus was calculated from the initial slope of the straight line of the obtained stress-strain plots and compressive strength was recorded as the maximum strength achieved before sample fracture. Detailed procedure is given below.

- i. Clamp calibration was made for compression clamp.
- ii. Test type was selected as “Compression”.
- iii. Then stress-strain controlled force mode was selected. Ramped force mode was chosen at isothermal temperature.
- iv. Isothermal temperature was adjusted to 37°C where soak time was approximately 5 minutes. Force ramp rate was selected as 0.1 N/min and the upper force limit was set as 18 N.
- v. Sample shape was chosen as round disc and then dimensions (thickness and diameter of discs) were entered.
- vi. Sample was placed on aluminum disc.
- vii. The compression machine was started to work.
- viii. Samples produced in disk form was compressed at a rate of 1 mm / min.
- ix. During compression, time in seconds, extension in mm and load in N were recorded.
- x. According to the results, stress (MPa) versus strain (p) graphs were plotted and analyzed.



Figure 3.6. Instron Universal Dynamic and Fatigue Systems device

3.5.6. *In-vitro* Degradation

Biodegradation behavior of PPF/VPES polymer and PPF/VPES/ β -TCP composite samples cured at 37°C, was followed via both weight change and pH change measurements in PBS buffer solution (pH=7.4) at 37°C. The reason behind the utilization of PBS buffer solution (pH=7.4) was to simulate the body environment during the entire analysis.

3.5.6.1. pH Measurements

Biodegradation behavior of body temperature cured PPF/VPES polymer and PPF/VPES/ β -TCP composites was investigated using 0.9 percent Na-Azide containing 1X Phosphate buffer saline at pH=7.4. During the experiment, bar shaped samples were put into the falcon tubes and PBS solution was introduced into each falcon tube (Figure 3.7). Each tube was put into a shaking water bath at 75 rpm and at 37°C. In the first two days, pH of the medium was measured every 12 hours. After two days, pH of the medium was measured every 24 hours. After one week, the pH of the medium was measured once a week. After every pH measurement, the buffer solution inside the falcon tube was refreshed carefully. Since the experiment was done duplicate, the average pH value for each sample was calculated and pH vs time graphs were plotted in order to simulate the pH change samples will cause inside the human body. The following procedure was applied.

- i. Bar shaped samples were cut into two uniform pieces (approximately 0.5 g).
- ii. Each sample was put into a 15 mL Falcon tube.
- iii. 10 mL of pH=7.4 PBS solution was put into each falcon tube with the sample.
- iv. For the first two days, pH of the samples was recorded for every 12 hours.
- v. After second day, pH of each sample was recorded for every 24 hours for 5 days.
- vi. After 1 week, pH change of each sample was recorded once a week.
- vii. These measurements were recorded for 84 days.



Figure 3.7. Experimental set-up of pH measurement method

3.5.6.2. Gravimetric Analysis Method

In order to perform biodegradation tests via weight loss measurements in PBS buffer solution (pH=7.4) containing 0.9 percent Na-Azide for the body temperature cured PPF/VPES/ β -TCP composites, initial mass of the each sample was recorded. After each sample was put into a separate test tube containing PBS buffer solution (pH=7.4) with 0.9 percent Na-Azide, tubes were placed into an incubator operating at a shaking rate of 75 rpm and at a temperature of 37 °C. Each sample was taken out of the incubator at the necessary time intervals and centrifuged in order to prevent loss of the material. PBS was taken out from the falcon tubes and the samples were washed with distilled water two times. Washed samples were dried and frozen overnight. Finally, final weight of each material was recorded. The following steps describe the procedure for weight loss analysis.

- i. All samples were cut into 4 equal parts. Initial weight of each sample part was recorded as W_0 (approximately 0.5 g).
- ii. 10 mL of 0.9 percent sodium azide containing 1X PBS solution (pH=7.4) was put into each falcon tube.
- iii. A known mass of the composite sample was put inside the 15 mL falcon tube with PBS solution in it.

- iv. Falcon tubes with the samples were incubated in a shaking water bath at 75 rpm. at 37 °C for the predetermined time intervals.
- v. After the incubation time, samples were taken out and put into centrifuge.
- vi. After the centrifugation. supernatants were decanted from falcon tubes.
- vii. Samples were washed with distilled water two times.
- viii. Samples were then dried and frozen overnight.
- ix. Samples were weighed and final mass of each sample was recorded.

At the end of the analysis, percent weight loss was calculated with Equation 2.6;

$$\% \text{ Weight loss} = \left| \frac{W_0 - W_1}{W_0} \right| \times 100 \quad (3.6)$$

4. RESULTS AND DISCUSSION

Upcoming section of this thesis contains the discussion about characterization of synthesized PPF, characterization of prepared PPF/VPES and PPF/VPES/ β -TCP composites with relevant references and examples.

4.1. CHARACTERIZATION OF PPF

4.1.1. Structural Analysis of PPF via FT-IR Spectroscopy

In this part of the study, firstly molecular characteristics of the synthesized PPF was analyzed via FT-IR spectroscopy for verification of the product. The FT-IR spectrum of the synthesized PPF (LMW) is shown in Figure 4.1. The chemical structure of the PPF pre-polymer was shown in Figure 3.1. Alcohol stretching band (O-H) at 3444 cm^{-1} region of the FT-IR spectrum was expected as the polymer is hydroxyl terminated. Also, alkyl stretching (C-H) peak on the 3080 cm^{-1} region, α -unsaturated ester carbonyl (C=O) stretching peak at 1732 cm^{-1} region, C=C stretching peak at 1645 cm^{-1} region and carboxylic acid (C-O) stretching peak at 1360 cm^{-1} region verify the molecular structure of the PPF product [41]. The HMW PPF pre-polymer showed a similar spectrum and therefore its FT-IR spectrum is not shown here.

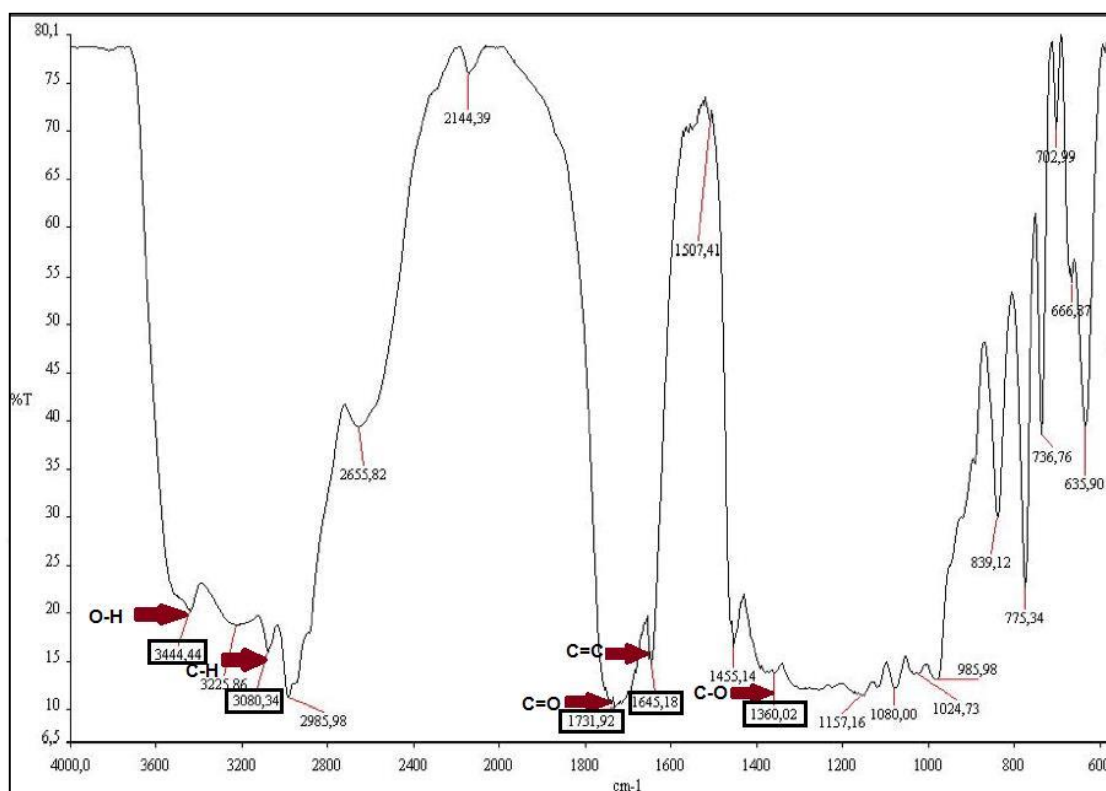


Figure 4.1. FT-IR Spectrum of the synthesized PPF pre-polymer.

4.1.2. Structural Analysis of PPF via Proton NMR ($^1\text{H-NMR}$) Spectroscopy

Further molecular structural analysis was performed on the synthesized PPF products via $^1\text{H-NMR}$ spectroscopy. The $^1\text{H-NMR}$ spectra of the synthesized low and high molecular weight PPF products are shown in Figure 2.10 and Figure 2.11 respectively with the peak assignments for the different type of protons on PPF structure. The formation of PPF polymer was verified by the observation of characteristic peaks associated with the $\text{CH}=\text{CH}$, CH_2 , CH_3 protons and CH protons of the PPF structure. The sharp peak around 1.2 ppm represents the methyl CH_3 protons, the multiplet peaks around 4.0-4.4 ppm indicate the CH protons of the propylene glycol backbone, the peak at around 5.15 ppm belongs to the methylene (CH_2) protons of the propylene glycol backbone again and the sharp peak at 6.7 ppm represents the $\text{CH}=\text{CH}$ protons of the PPF backbone in both spectra. As can be seen in these spectra, some peaks were identified as not belonging to the PPF product such as multiplet peaks in the 3.5-4.0 ppm region which may belong to CH_2 protons of diethyl ether utilized in the purification step. The peak at around 7.24 ppm

should indicate the proton residue of the deuterated chloroform (CDCl_3) which was utilized as the solvent during proton NMR analysis.

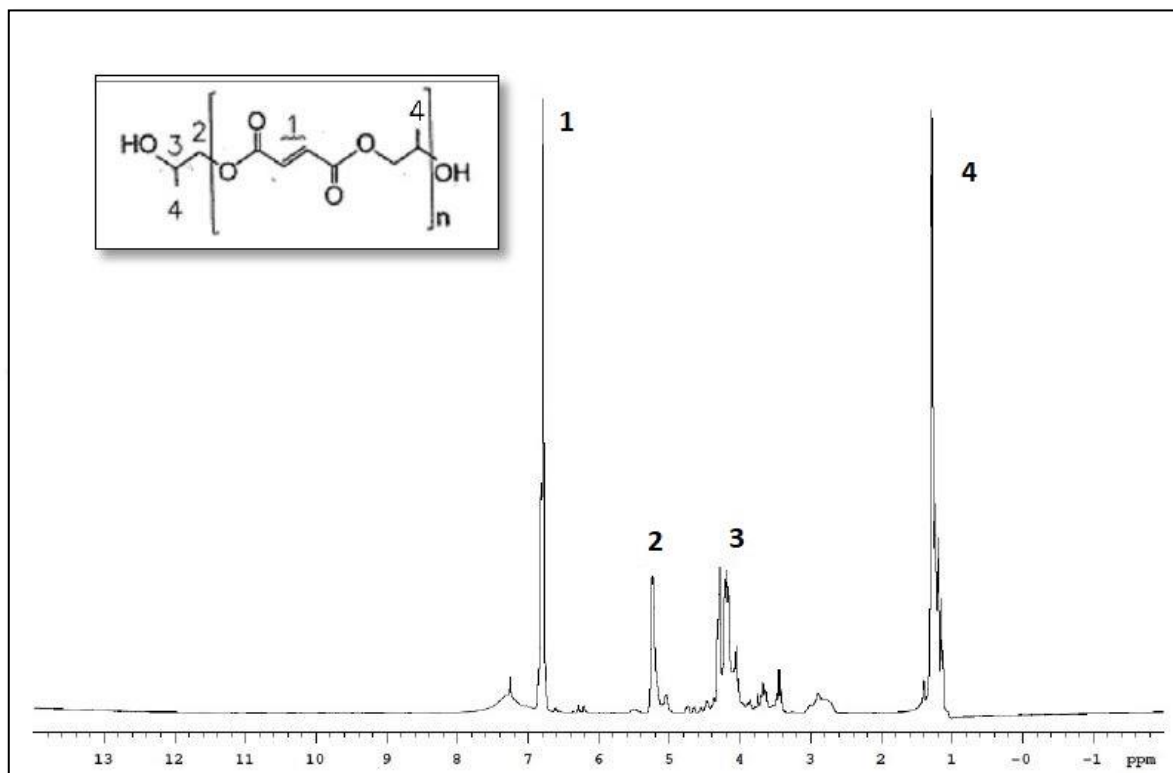


Figure 4.2. ^1H -NMR spectrum of LMW PPF

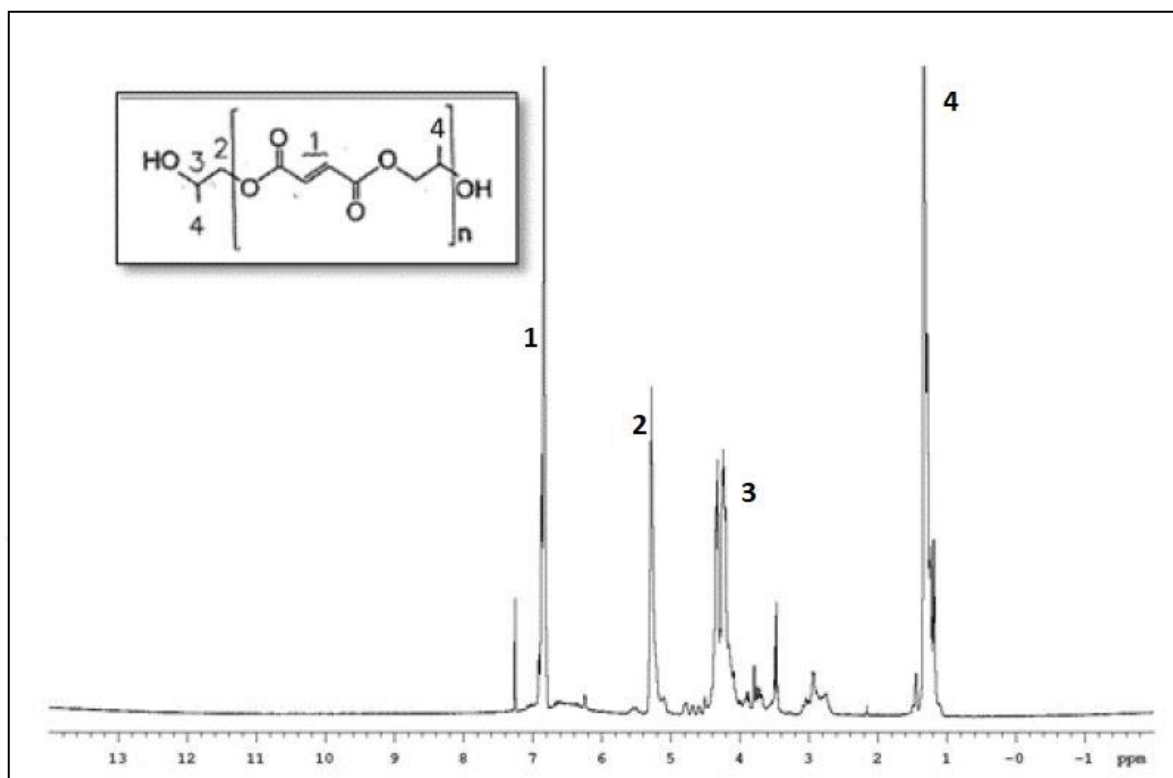


Figure 4.3. $^1\text{H-NMR}$ spectrum of HMW PPF

Moreover, ratio of the integral of the peak representing the vinyl protons ($-\text{CH}=\text{CH}-$) (peak 1) over the integral of the peak representing the methyl (CH_3) protons (peak 4) was calculated for each product and this data is presented in Table 4.1. For the PPF repeating unit structure, there are two vinyl protons ($-\text{CH}=\text{CH}-$) against three methyl protons (CH_3). However, methyl protons (CH_3) on the end of the polymer chain has a decreasing effect on the ratio of the number of vinyl protons over the number of methyl protons. When the molecular weight of PPF increases, the number of polymer chains, and the number of polymer chain ends (propylene glycol units) decreases but the chain length increases. That is the reason why, ratio of total amount of vinyl protons over methyl protons increases with increasing molecular weight. As can be seen in Table 4.1, the ratio of integral of peak 1 ($-\text{CH}=\text{CH}-$) over integral of peak 4 (CH_3) increases from 1.36 for the LMW PPF to 2.49 for the HMW PPF which is in agreement with the molecular weight data of these products that will be presented in the following section.

Table 4.1. Integral ratios of peak 1 which represents the -CH=CH- protons over peak 4 which represents the methyl (CH₃) protons of PPF polymer

Synthesized PPF	$\frac{\int \text{Peak 1}}{\int \text{Peak 4}}$
Low Molecular Weight (LMW) PPF	1.36
High Molecular Weight (HMW) PPF	2.49

4.1.3. Molecular Weight of PPF

The number average and weight average molecular weight and polydispersity index (PDI) of the synthesized PPF products were obtained via gel permeation chromatography analysis. The data obtained is presented in Table 4.2. The increase of the reaction time from 3 hours at 145°C to 8 hours, and then from 1 hour at 180°C to 5 hours and the addition of propylene glycol excess stepwise with the use of 0.2wt percent hydroquinone resulted in an increase in number average molecular weight (M_n) from 1190 g/mol to 2558 g/mol and from 1678 g/mol to 4768 g/mol in weight average molecular weight (M_w). As a result of the increased reaction time, the PDI also increased from 1.41 to 1.86 as expected. The HMW PPF and VPES mixture (PPF/VPES(wt)=70/30) was able to cure and solidify in the presence of 0.3wt percent BP and 0.06wt percent N,N-DMT at 37° C whereas cure of the LMW PPF with the VPES comonomer with the use of BP initiator and N,N-DMT catalyst was not possible. Thus the HMW PPF was used to prepare the body temperature cured β -TCP composites which was designed to be used in injectable bone cement. The LMW PPF was used to prepare the high temperature cured β -TCP composites to demonstrate the use of these materials in preformed forms as a bone replacement. The increase in molecular weight increased the viscosity of the PPF product significantly, the HMW PPF product was nearly solid at room temperature. Obtained GPC data (M_w , M_n and PDI) in this study is remarkably close to molecular weight data of PPF prepared by Yazemski et al [42].

Table 4.2. Molecular weight data of the synthesized PPF products as determined via GPC.

Synthesized PPF	M_n (g/mol)	M_w (g/mol)	DI
Low Molecular Weight (LMW) PPF	1190	1678	1.410
High Molecular Weight (HMW) PPF	2558	4768	1.8644

4.2. CHARACTERIZATION OF PPF/VPES POLYMER AND PPF/VPES/ β -TCP COMPOSITES

The body temperature cured PPF/VPES polymer and PPF/VPES/ β -TCP composites were characterized via cross-link density analysis, differential scanning calorimetry analysis (DSC), thermal gravimetric analysis (TGA) and equilibrium water content analysis. Surface hydrophilicity was investigated via determining contact angle with water and surface characteristics were investigated by Scanning Electron Microscopy (SEM) analysis. In addition, compressive properties were determined by compression tests and in-vitro degradation behavior was analyzed for all the composite formulations. For the high temperature cured PPF/VPES polymer and PPF/VPES/ β -TCP composites on the other hand, only DSC analysis will be presented to demonstrate the successful cure of these materials applying the high temperature cure cycle and therefore the potential use of the composites in preformed forms as a bone substitute however further characterization will not be presented.

Images of the body temperature cured PPF/VPES polymer and PPF/VPES/ β -TCP composites (with 5,10,15,20 wt percent β -TCP) are presented in Figure 4.4. The image the high temperature cured PPF/VPES (70/30)-10 percent β -TCP composite is given in Figure 4.5. The yellow brown color of the body temperature cured materials should result from the use of N,N DMT catalyst.

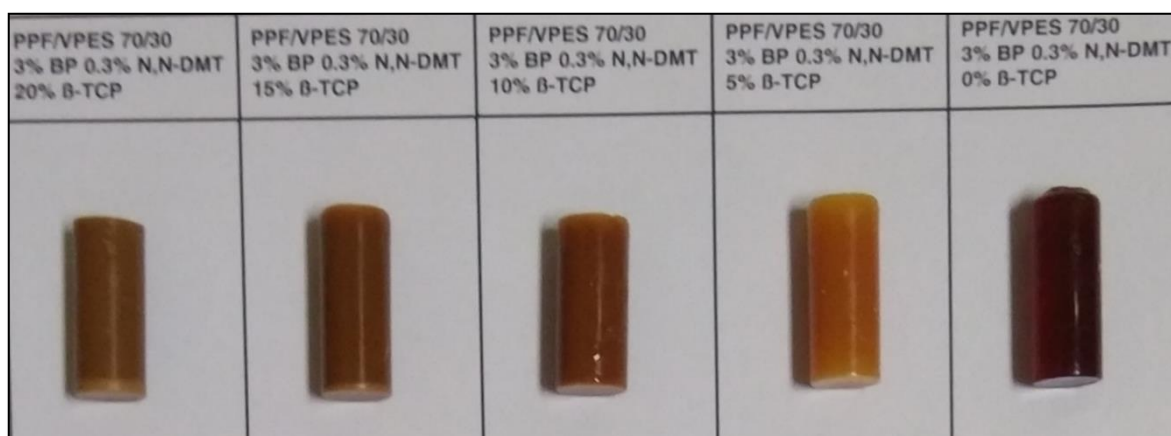


Figure 4.4. Images of the body temperature cured PPF/VPES polymer and PPF/VPES/ β -TCP composites (with 5,10,15,20 wt % β -TCP)



Figure 4.5. Image of thermal cured PPF/VPES (70/30)-10% β -TCP composite.

4.2.1. DSC Analysis

DSC thermograms of thermally cured PPF/VPES/ β -TCP composites are shown in Figure 4.6. When these thermograms are analyzed, exothermic step changes are observed between 90 and 110 °C which can be explained by the evaporation of the water molecules held by β -TCP molecules. The hydrophilicity of β -TCP inorganic filler is quite high [43]. In addition, the polar groups on the PPF/VPES matrix increases the hydrophilicity of the material. Also, the absence of exothermic peaks in these thermograms indicates that the

cure reaction of the composites under the applied high temperature cure cycle conditions was complete.

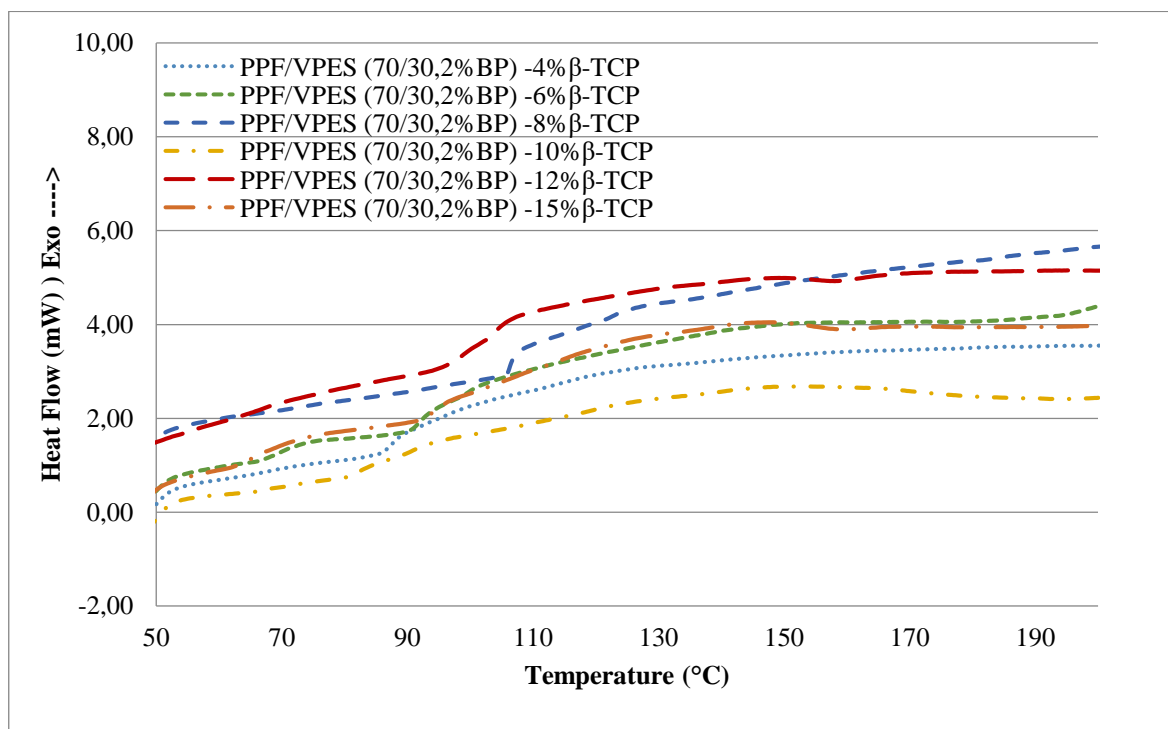


Figure 4.6. DSC thermograms of thermally cured PPF/VPES/ β -TCP composites (2 % BP)

DSC thermograms of body temperature cured PPF/VPES and PPF/VPES/ β -TCP (5, 10, 15, 20 wt percent β -TCP) materials cured with 3wt percent BP and 0.3wt percent N', N'-DMT, for the first and second heating are shown in Figure 4.7(a) and (b) respectively. The exothermic increase of the heat flow after 100 °C in Figure 4.7(a) indicates the evaporation of the water molecules held by both PPF/VPES matrix and β -TCP filler. In addition to the polar groups of the PPF/VPES matrix, β -TCP has highly hydrophilic structure and it has a high capacity to absorb water [43]. Apart from the minor exothermic peak at 137 °C on Figure 4.7 (a) for the PPF/VPES (70/30) –15 percent β -TCP sample, the absence of major exothermic peaks on these thermograms indicates that the cure reaction of PPF/VPES at 37 °C in the presence of β -TCP with the use of 3 percent BP and 0.3 percent N', N'-DMT was completed. The exothermic increase of the heat flow after 100 °C as well as the the minor exothermic peak at 137 °C for the 15 percent β -TCP sample, were disappeared for the second heating (Figure 4.7 (b)) as expected. Moreover, endothermic changes that can be

associated with the glass transition of these materials were not observed in these thermograms for the second heating.

Finally, the minor stepwise heat flow increase after 169 °C can be attributed to the degradation of the side groups of the PPF/VPES network structure.

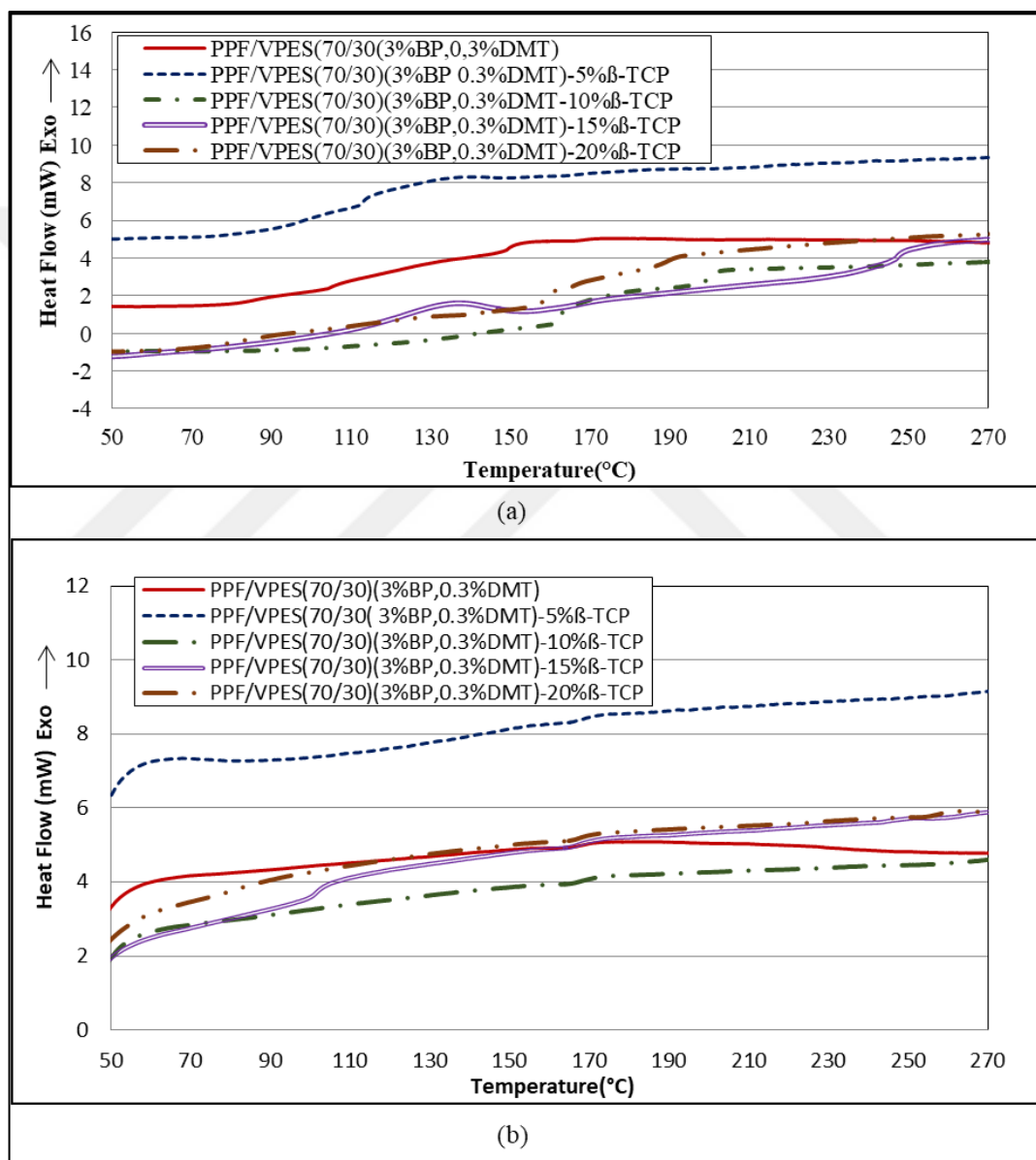
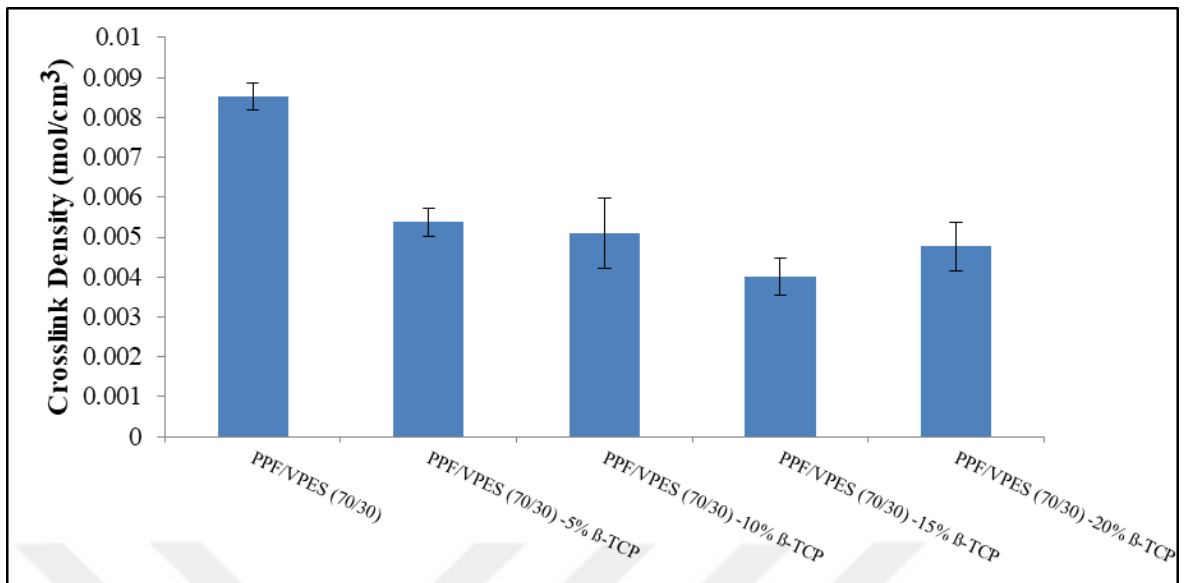


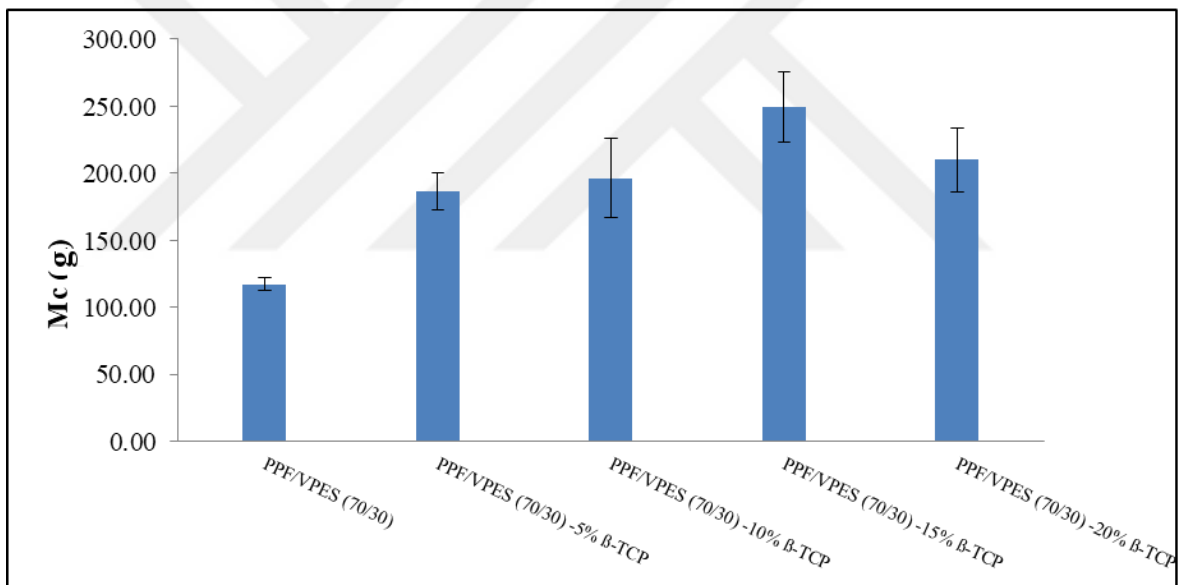
Figure 4.7. DSC thermograms of body temperature cured PPF/VPES polymer and PPF/VPES/β-TCP composites (a) first heating cycle (b) second heating cycle

4.2.2. Cross-link Density Analysis

Cross-link density and molecular weight between cross link (M_c) values for the 37 °C cured PPF/VPES polymer and PPF/VPES/ β -TCP composites are listed in Table A.1 (Appendix A). The column graphs for cross-link density and M_c values are also presented in Figure 4.8 and 4.9 respectively. As can be seen from these figures, the cross-link density generally decreases with increasing β -TCP content and thus molecular weight between cross-link values (M_c) increases with increasing β -TCP amount. The data shows that, cross-link density value of the PPF/VPES polymer ($8.5 \times 10^{-3} \text{ mol/cm}^3$) decreases to approximately its half value for the PPF/VPES - 15 percent β -TCP composite ($4.0 \times 10^{-3} \text{ mol/cm}^3$). This result can be explained by the decrease of the mobility of PPF polymer chains because of the increase in viscosity with addition β -TCP and thus the decrease in ability of PPF polymer to react with VPES comonomer. Similarly, Jayabalan et al. prepared composites of poly(propylene fumarate-co-caprolactone diol) reinforced with Kevlar fiber and hydroxy apatite (HA) and reported that the cross-link density of the poly(propylene fumarate-co-caprolactone diol) matrix decreased with the addition of Kevlar fiber and HA. The authors explained that the filler materials formed a barrier for the reaction of the unsaturated polyester with the vinyl comonomer [44]. In addition, cross-link density value of body temperature (37 °C) cured neat PPF/VPES (70/30) polymer ($8.5 \times 10^{-3} \text{ mol/cm}^3$) was quite close to high temperature cured PPF/VPES (70/30) polymer (cured with 3 percent BP initiator) ($8.6 \times 10^{-3} \text{ mol/cm}^3$). This result indicates that the cure reaction of the PPF/VPES (70/30) composition in the presence of 3 percent BP and 0.3 percent N,N- DMT at 37 °C is as effective as the cure reaction applying the high temperature cure conditions using again 3 percent BP [45].



(a)

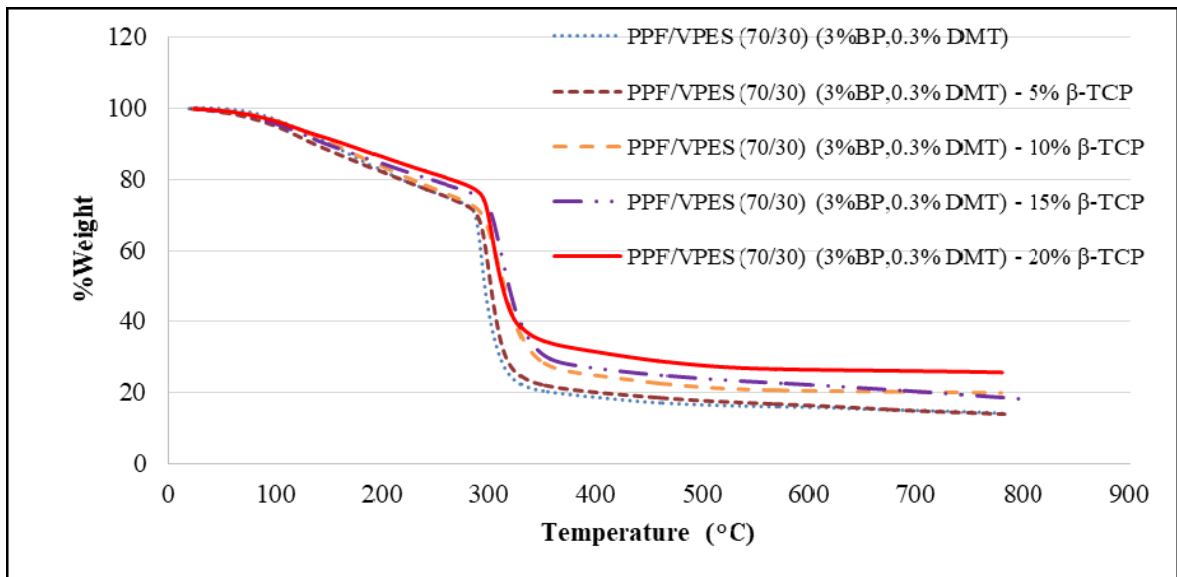


(b)

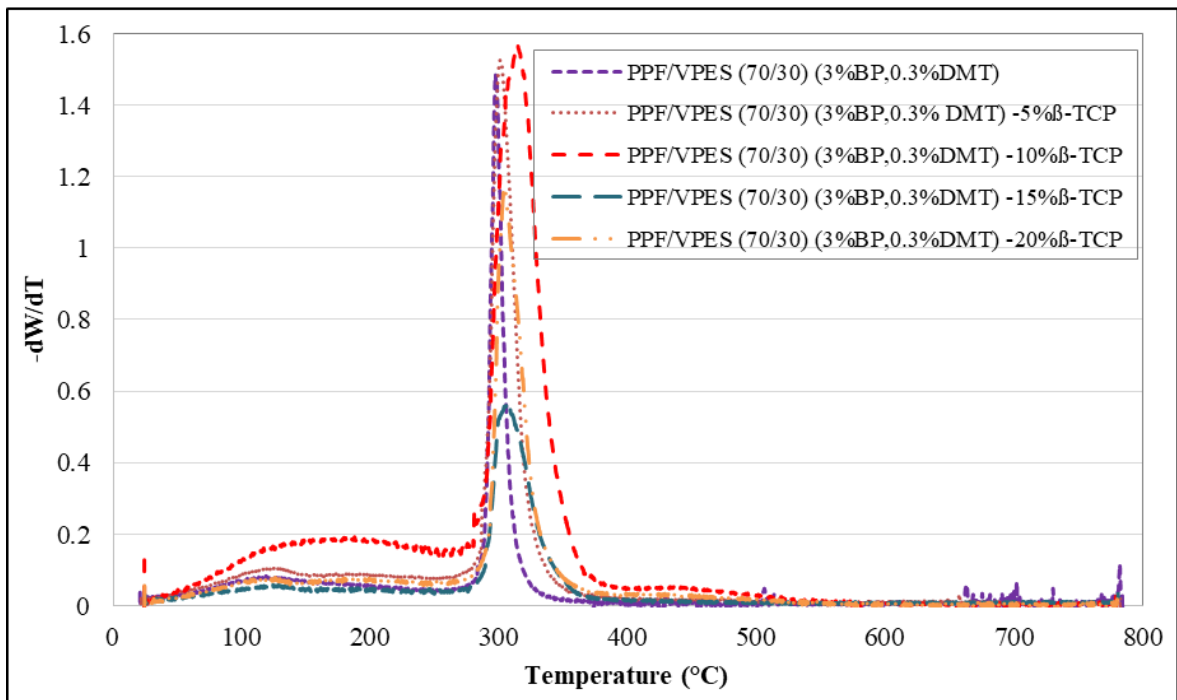
Figure 4.8. (a) Cross-link density and (b) molecular weight between cross-links (M_c) values of body temperature (37 °C) cured PPF/VPES polymer and PPF/VPES/ β -TCP composites (using 3% BP and 0.3% N, N- DMT)

4.2.3. Results of TGA

Thermal gravimetric analysis results of PPF/VPES and PPF/VPES/ β -TCP composites cured with 3 percent BP and 0.3 percent N, N-DMT at 37°C are shown in Figure 4.9. During the analysis, both percent weight vs temperature plots (Figure 4.9(a)) and derivative weight loss (-dW/dT) vs temperature plots (Figure 4.9(b)) were constructed. In Figure 4.9(a), linear weight loss that starts after 100 °C for both the PPF/VPES polymer and PPF/VPES/ β -TCP composites indicates the evaporation of water molecules absorbed by the PPF/VPES matrix and β -TCP filler. The major weight loss observed between 290-330 °C can be assigned to the one step degradation of PPF/VPES cross-linked matrix structure. A recent study also reported that the degradation of cross-linked PPF network starts at 285 °C and occurs as a one stage degradation [34]. After the main degradation, char residue at 800°C which is 14 percent for PPF/VPES increases with increasing β -TCP content for the composites. Similarly, in a study on PLLA/ β -TCP composites, char residue after main degradation was reported to increase with increasing β -TCP content of the composites according to thermal gravimetric analysis [43]. The temperature of maximum weight loss was 297°C for the PPF/VPES polymer , 300°C for the percent 5 β -TCP composite , 315°C for the percent 10 β -TCP composite, 309°C for the percent 15 β -TCP composite and finally 305°C for the 20 β -TCP composite.(Figure 4.9(b)). Thus, the main degradation temperature increased with the introduction of β -TCP filler. Similarly the main degradation temperature of PPF-Hydroxy apatite (HA) composites was reported to increase with increasing HA content (20 °C increase for the 30 percent HA) [39]. Thus thermal gravimetric analysis showed the successful incorporation of β -TCP filler in the composites and that the thermal stability of the prepared composites increased with β -TCP filler as expected.



(a)



(b)

Figure 4.9 (a) Percent weight vs temperature (b) -derivative weight (-dW/dT) vs temperature graphs of body temperature cured PPF/VPES polymer and PPF/VPES/β-TCP composites.

4.2.4. Results of SEM Analysis

The fracture surfaces of the body temperature cured PPF/VPES/ β -TCP composites were analyzed to characterize the β -TCP filler content in the PPF/VPES matrix. The SEM images of the PPF/VPES/ β -TCP composites with 5, 10, 15 and 20wt percent β -TCP at 2000X magnification are presented in Figure 4.10. As can be seen the PPF/VPES matrix has a non-porous structure. Only a few β -TCP particles can be observed in the SEM image of the 5 percent β -TCP composite (Figure 4.10(a)), whereas the β -TCP particles seem to be well dispersed on the matrix at higher β -TCP content (10-20 percent). Some aggregates seem to form for the 15 percent and 20 percent β -TCP composites (Figure 4.10(c, d)). Holes formed through the fracture of the β -TCP particles can also be observed on the fracture surface of the 20 percent β -TCP composite (Figure 4.10(d)). Overall it can be said that the β -TCP particles are well dispersed in the PPF/VPES matrix for the 10 percent, 15 percent and 20 percent β -TCP composites.

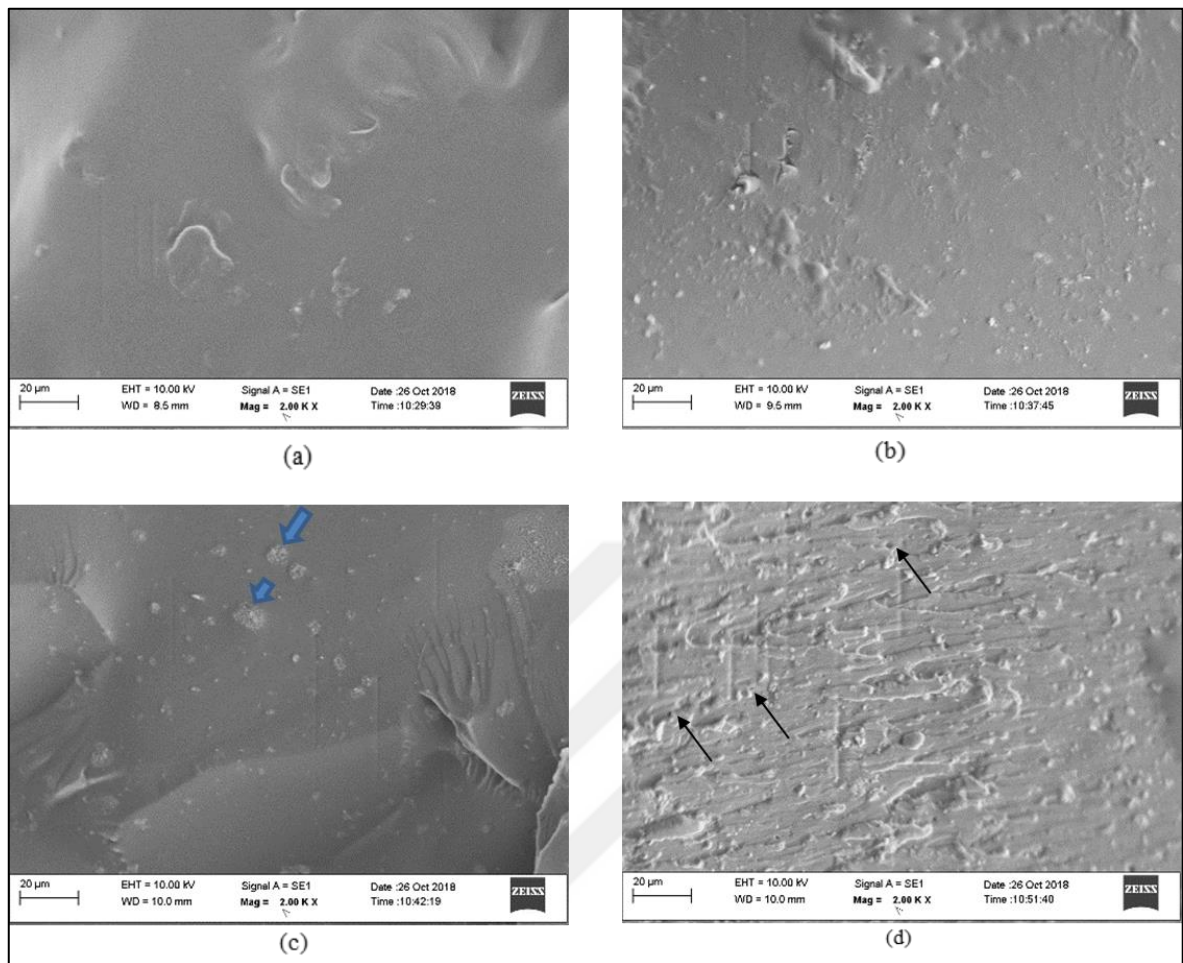


Figure 4.10. SEM images of body temperature cured PPF/VPES/ β -TCP composites with (a) 5% β -TCP (b) 10% β -TCP (c) 15% β -TCP (d) 20% β -TCP at 2000X magnification

4.2.5. Equilibrium Water Content (EWC) Analysis

Equilibrium water content of a polymeric material which can be calculated by the amount of water absorbed by 100 grams of the polymer is an indication of the dimensional stability of the material. As the equilibrium water content increases, the extent of dimensional change increases [46]. Equilibrium water content values of body temperature cured PPF/VPES polymer and PPF/VPES/ β -TCP composites cured with 3 percent BP and 0.3 percent N', N'DMT are listed in Table A.2. (Appendix A). Column graphs of the EWC data are presented in Figure 4.11. An examination of Figure 4.11 indicates a decrease in EWC for the 5 percent-10 percent and 15 percent β -TCP containing composites and an increase for the 20 percent β -TCP composite as compared to the PPF/VPES polymer. In a study on composites based on PPF cured with poly(ethylene glycol)-dimethacrylate (PEG-

DMA) and β -TCP, it has been reported that the equilibrium water content of neat PEG-DMA/PPF material increased from 21.7 percent to 22.3 percent with increasing PEG-DMA/PPF double bond ratio from 0.38 to 1.88 and the equilibrium content value for the composite samples containing 3 percent β -TCP decreased as compared to neat PEG-DMA/PPF polymer [46]. The EWC values of these materials were reported to be between 18 percent and 25 percent depending on the PEG-DMA/PPF double bond ratio. The EWC value of the body temperature cured PPF/VPES polymer (17.4 ± 36 percent) was found to be lower than the values reported for the PEG-DMA/PPF polymers. The decrease in equilibrium water content with the introduction of β -TCP filler for the 5, 10, 15 percent β -TCP composites can be explained as the incapability of β -TCP molecules to absorb water as the PPF/VPES matrix structure. On the other hand, the increase in EWC for the 20 percent β -TCP composite can be explained by the relatively lower dispersion of β -TCP content in the PPF/VPES matrix and a weak interaction of β -TCP particles with the PPF/VPES polymer. In another study, according to Jayabalan et al., the EWC value of a composite based on poly(propylene fumarate-co-caprolactone diol)/N-vinyl pyrrolidone (PPFPL/NVP) and hydroxyapatite (HA) (4.8 percent) decreased when compared to the EWC value of the neat PPFPL/NVP polymer (6.25 percent) [40].

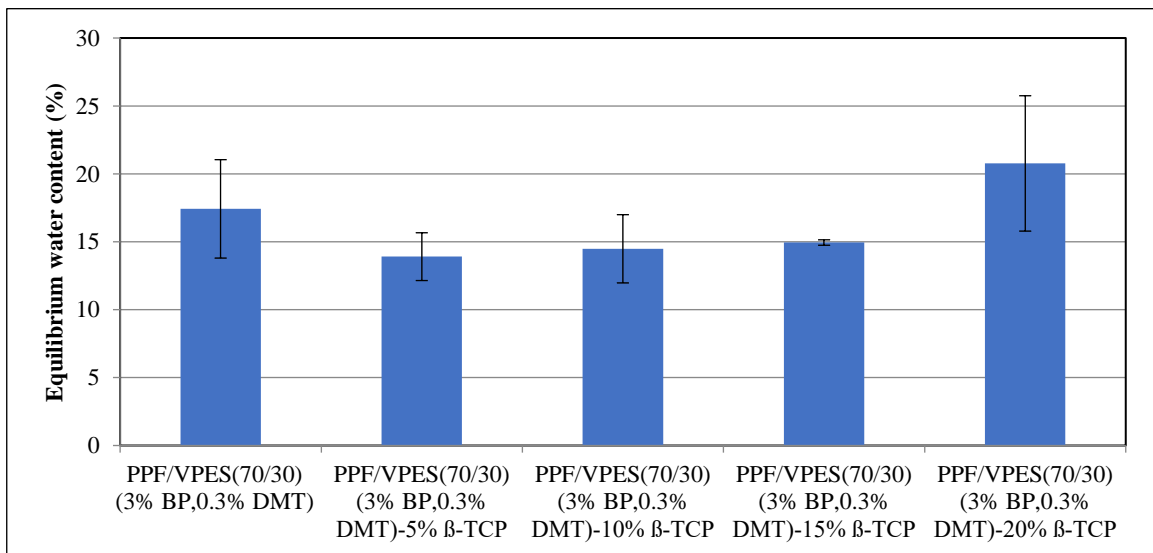


Figure 4.11. Equilibrium water content values of body temperature cured PPF/VPES polymer and PPF/VPES/ β -TCP composites

4.2.6. Contact Angle with Water: Surface Hydrophilicity

Average values of contact angle with water (at the end of 30th second) for body temperature cured PPF/VPES (70/30) polymer and PPF/VPES (70/30) - β -TCP composites are listed in Table A.3. (Appendix A) and column graphs of these values are shown in Figure 4.12. As can be seen from this data, the contact angle with water for the PPF/VPES polymer decreased with the addition of β -TCP into the system. This result can be explained by the more hydrophilic structure of β -TCP due to its dense phosphate groups as compared to the PPF/VPES polymer matrix. Reported results indicate that materials with hydrophilic surfaces having contact angle with water values of 50° or lower have higher cell attachment rate when compared with hydrophobic surfaces. Thus, composites with 10 percent - 20 percent β -TCP are expected to have a higher cell attachment as compared to the PPF/VPES polymer. Cell proliferation studies by MTS assay of these materials presented in another study, showed a higher cell attachment for the 20 percent β -TCP composite as compared to the neat PPF/VPES polymer on 21st and 28th days after cell incubation [47]. According to the study of Lee et al., similar to our results, surface hydrophilicity of PPF/Hydroxy apatite (HA) composites increased and therefore contact angle with water decreased with increasing HA content [35]. Contact angle value at the 30th second for PPF was reported as $68.9 \pm 8.2^\circ$ and this value decreased with increasing HA content and reaching to its minimum value at 30 percent HA content which was $34.9 \pm 3.7^\circ$ [35]. The contact angle with water at the 30th second for the body temperature cured PPF/VPES (70/30) polymer which was found as $(59.6 \pm 1.2^\circ)$ in our study, is lower than the value reported for the PPF polymer in the related study. This can be explained by the more hydrophilic structure of the PPF/VPES copolymer as compared to the PPF polymer.

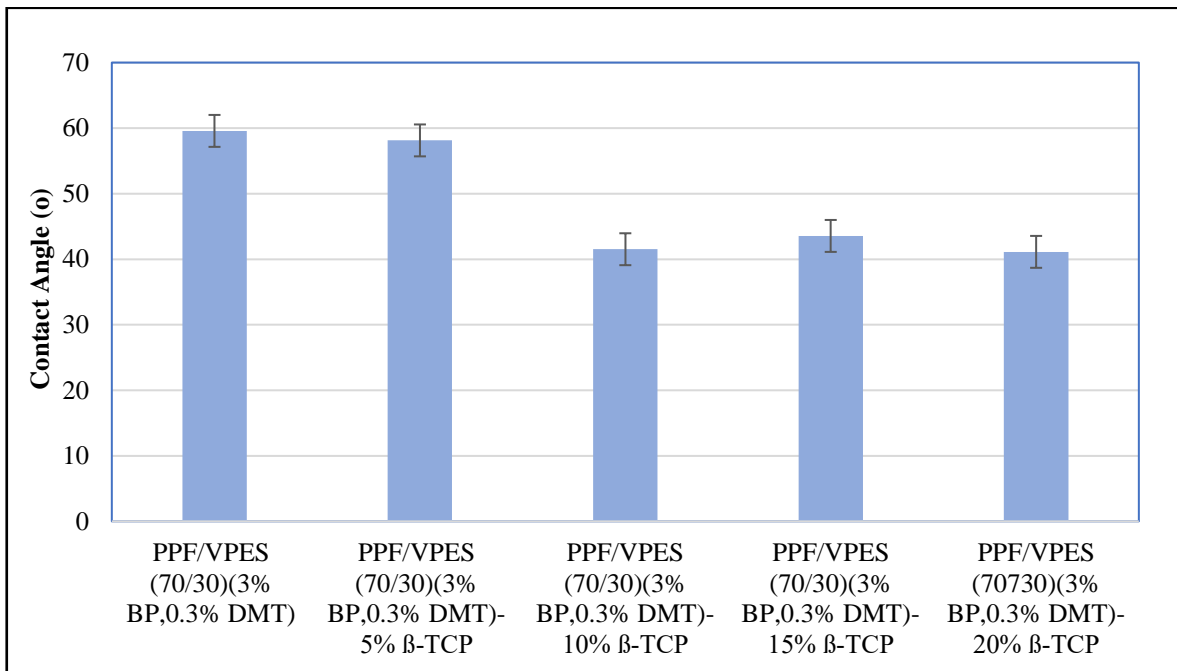


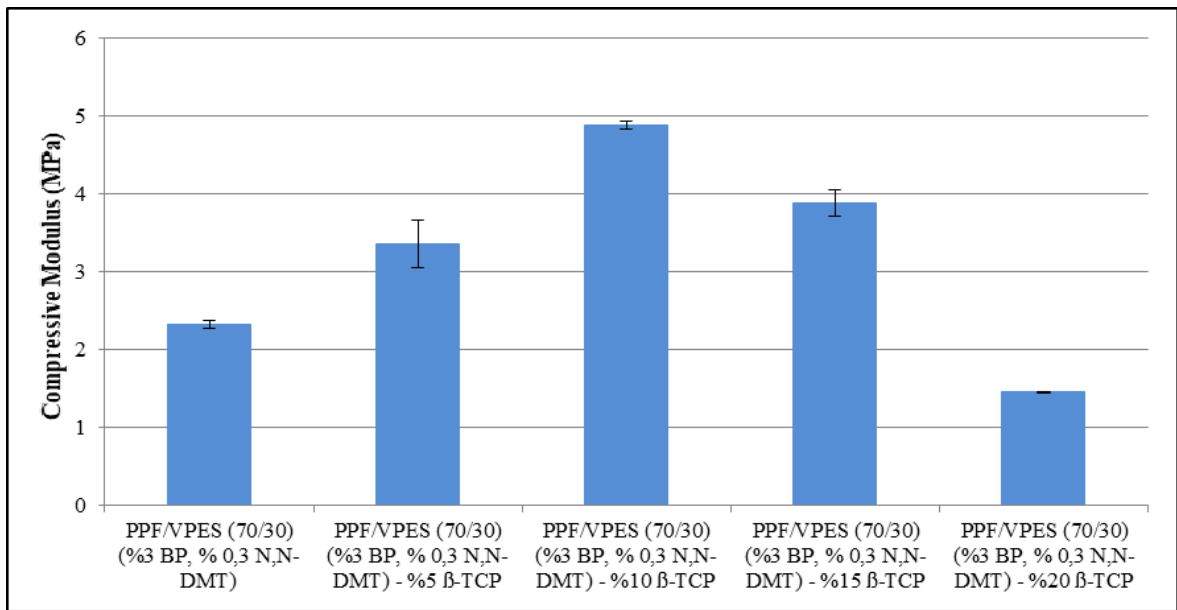
Figure 4.12. Contact angle with water for the body temperature cured PPF/VPES polymer and PPF/VPES/ β -TCP composites at 30th second

4.2.7. Compressive Properties

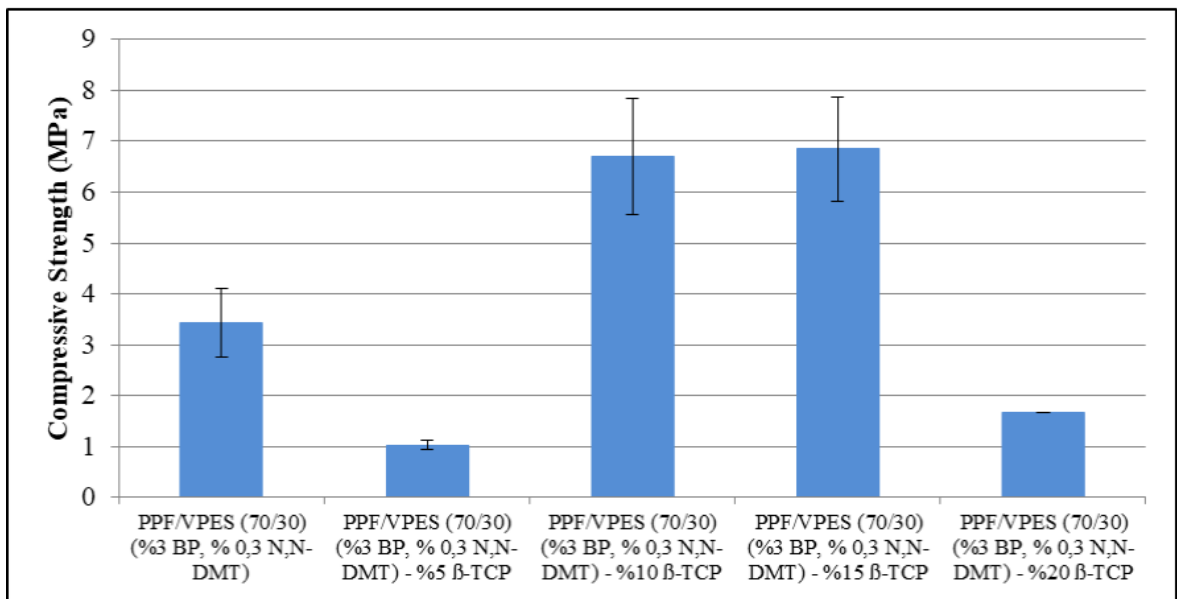
Compressive modulus and strength values of body temperature cured PPF/VPES polymer and PPF/VPES (70/30) - β -TCP composites are tabulated in Table A.4. (Appendix A). The column graphs of the compressive modulus and strength values of these materials are presented in Figure 4.13. Compressive modulus values of the PPF/VPES - 5 percent-20 percent β -TCP composites changed between 1.45 ± 0.01 MPa and 4.89 ± 0.05 MPa, and their compressive strength values were in the range of 1.03 ± 0.09 MPa - 6.86 ± 1.02 MPa. Compressive modulus reached the maximum value at 10 percent β -TCP content, increased for the 15 percent β -TCP composite as compared to the PPF/VPES polymer. However, compressive modulus of the 20 percent β -TCP composite was significantly decreased as compared to that of PPF/VPES polymer. The compressive strength reached maximum values at 10 percent and 15 percent β -TCP content (approximately twice the compressive strength value of the PPF/VPES polymer) and decreased for the 20 percent β -TCP composite to about half of the compressive strength value of the PPF/VPES polymer. This decrease in both compressive modulus and strength at 20 percent β -TCP content can be

explained by the formation of aggregates of β -TCP particles or pellets which act as weak-spots on the material. Thus, till 15 percent β -TCP content, the β -TCP particles are more homogenously dispersed throughout the PPF/VPES matrix and act to increase both the modulus and strength however above 15 percent, at 20 percent β -TCP content the filler particles form more aggregates (Figure 4.10) which form defect points on the composite structure.

At this point, it must be noted that both the compressive modulus and strength values of the PPF/VPES polymer cured with 3 percent BP and 0.3 percent N,N-DMT at 37°C decreased significantly as compared to the compressive modulus (836.0 ± 6.2 MPa) and strength (118.6 ± 24.5 MPa) values of the PPF/VPES polymer cured with 3 percent BP applying the high temperature cure cycle. As discussed previously in section 4.2.2, the cross-link density of the body temperature PPF/VPES polymer did not decrease significantly as compared to the high temperature cured PPF/VPES polymer. Thus this significant decrease in compressive modulus and strength of the body temperature cured samples as compared to those of high temperature cured samples may be attributed to the plasticization effect of the lower molecular weight monomer or VPES homopolymer that was not able to incorporate into the network structure during cure at body temperature. For the high temperature cured PPF/VPES samples, it is believed that all components of the system are connected in the network structure and such a plasticization effect was not observed.



(a)



(b)

Figure 4.13. Column graphs of (a) Compressive modulus and (b) Compressive strength of body temperature cured PPF/VPES polymer and PPF/VPES/ β -TCP composites

In a study by Cai et al., compressive properties of PPF/NVP/(CaSO₄/ β -TCP) composites increased with decreasing NVP/PPF and CaSO₄/ β -TCP molar ratios. Compressive strength and compressive modulus values of these composites at changing formulations were reported to be in the range of 12-62 MPa and 290-1149 MPa respectively [39]. In a similar study on composites based on PPF cross-linked with polyethylene glycol- dimethacrylate

(PEG-DMA) reinforced with β -TCP, the compressive strength of PEG-DMA/PPF material was reported to be between 5.9 ± 1.0 and 11.2 ± 2.2 MPa and compressive modulus values were reported to be in the range of 30.2 ± 3.5 - 58.4 ± 6.2 MPa for the DMA/PPF double bond ratios in between 0.38 and 188 and both compressive modulus and strength values were reported to increase with the addition of 3 percent β -TCP into the system [35]. In our study, the compressive modulus and strength values of the high temperature cured PPF/VPES polymer was found to be in the range of values reported for the PPF/NVP polymers and higher than the values reported for the PEG-DMA/PPF polymers whereas the compressive modulus and strength values of the 37 °C cured PPF/VPES polymer were lower than those of the two other PPF systems. Also in our study, the addition of β -TCP filler improved both the compressive modulus and strength till a certain content which is in agreement with the reference studies.

4.2.8. Biodegradation Rate (*In-vitro* degradation)

4.2.8.1. Results of Gravimetric Analysis

Figure 4.14 shows the weight loss data (percent weight loss versus time graphs) of the body temperature cured PPF/VPES polymer and PPF/VPES/ β -TCP composites that took place in PBS buffer solution (pH= 7.4) at 37 °C. As can be seen from the plots, the samples lost weight to a higher extent in the first 7 days and the rate of weight loss decreased after 7 days. It is postulated that the fast weight loss that occurred in the first 7 days occurred due to release of poly(vinyl diethyl ester) (PVPEs) chains that were not incorporated into the network structure and that the slower weight loss afterwards occurred due to the hydrolytic degradation of the PPF/VPES network. An examination of Figure 4.14 indicates that the addition of the 5 to 20 percent of β -TCP filler did not affect the weight loss profile and therefore degradation rate of the PPF/VPES polymer significantly. The percent weight loss values of the PPF/VPES polymer and PPF/VPES/ β -TCP composites at the end of 7th and 84th days are also tabulated in Table 4.1. Percent weight loss of the PPF/VPES material at the end of 7th day was 22.9 percent and those of the (5 percent-20 percent) β -TCP composites were in the range of 22.5-27.3 percent. Percent weight loss at the end of 84th day for PPF/VPES material was 43.3 percent which was between 42.4-45.0 percent for the (5 percent-20 percent) β -TCP composites. Apart from 10 percent β -TCP composite,

for all the other compositions the β -TCP composites exhibited only slightly higher weight loss and therefore a higher degradation rate as compared to the PPF/VPES polymer. If the decrease in cross-link density of PPF/VPES materials with the introduction of β -TCP is taken into consideration, β -TCP composites may be expected to have a higher degradation rate and therefore to be exposed to a significantly higher weight loss. The obtained results on the other hand can be explained by the lower degradation rate of β -TCP as compared to that of PPF/VPES polymer and therefore the compensation of the two opposite effects. In a study by Peter et.al on PPF - β -TCP composites [38], for the in-vitro degradation studies for 12 weeks, it has been reported that the addition of β -TCP filler improved mechanical properties of the polymer matrix but did not affect the weight loss profiles and therefore the degradation rate similar to our results.

In another related study, analysis of the degradation behavior of PPF/NVP/(CaSO₄/ β -TCP) composites showed that weight loss during degradation (degradation rate) decreased with increasing molecular weight of PPF, decreasing NVP/PPF and CaSO₄/ β -TCP molar ratios. This result was explained by slower degradation of beta-TCP relative to CaSO₄. The highest weight loss at the end of 6 weeks was reported as 14.72 percent in the same study [39]. Still in another study, the effect of β -TCP filler on the in -vitro biodegradation rate of PPF cross-linked with poly(propylene fumarate diacrylate) (PPF-DA) macromer was investigated [40]. The presence of 33 percent β -TCP for the PPF/ PPF-DA / β -TCP composite resulted in a considerably higher weight loss in the first 40 weeks as compared to the matrix polymer

The weight loss of the PPF/VPES/ β -TCP composites with 5-20 percent β -TCP content at the end of 12 weeks was found to be in the range of 40-45 percent which shows that the PPF/VPES polymer matrix cured at body temperature that was developed in this study degrades at a higher rate as compared to the PPF/Vinyl pyrrolidone (VP) and PPF/poly(propylene fumarate diacrylate) (PPF-DA) materials reported in literature.

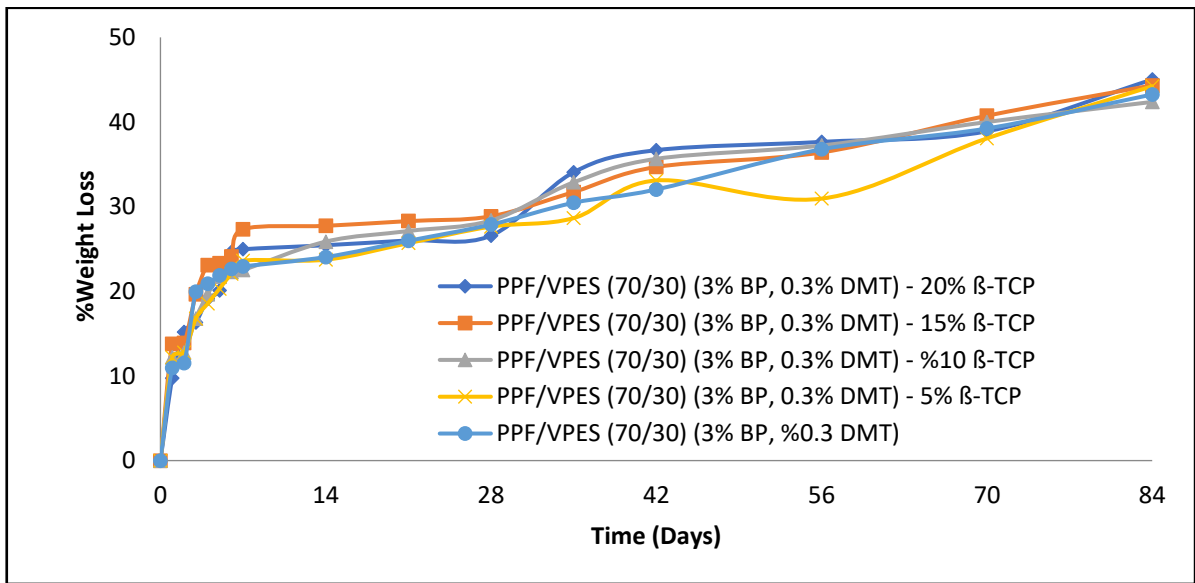


Figure 4.14. Percent weight loss vs time graphs of body temperature cured PPF/VPES polymer and PPF/VPES/ β -TCP composites

Table 4.1. Percent weight loss values of body temperature cured PPF/VPES polymer and PPF/VPES/ β -TCP composites at the end of 7th and 84th days.

Sample	Percent Weight loss at the end of 7 th day (%)	Percent weight loss at the end of 84 th day (%)
PPF/VPES – 0% β-TCP	22.94	43.25
PPF/VPES – 5% β-TCP	23.62	44.25
PPF/VPES – 10% β-TCP	22.51	42.38
PPF/VPES – 15% β-TCP	27.34	44.33
PPF/VPES – 20% β-TCP	24.97	45.01

4.2.8.2. Results of pH Measurements

Since the degradation products of the PPF/VPES network structure contains acidic species such as fumaric acid, the pH change in PBS buffer solution (pH=7.4) for the body temperature cured PPF/VPES/ β -TCP materials was investigated at 37 °C. There should be

a linear proportionality between degradation rate and decrease in pH because of the acidic degradation products of the PPF/VPES material. Thus, there is an expected pH drop during degradation. pH change in PBS buffer solution versus time plots of body temperature cured PPF/VPES polymer and PPF/VPES/ β -TCP composites are shown in Figure 4.15. As can be seen from this figure, pH decreased to a significant extent in the first 7 days and afterwards pH decreased at a slower rate. For the PPF/VPES material, the initial pH value (7.4) dropped approximately to 4.25 on the 7th day and then decreased at a slower rate with a final pH value at the end of 84 days of 3.5. For the composites, the pH value of 5, 10 and 15 percent β -TCP composites at the end of 7th day was approximately 5.46, and that of 20 percent β -TCP containing composite was 5.19 and again the pH values decreased at a slower rate afterwards. The final pH values at the end of 84th day for the 5, 10, 15 and 20 percent β -TCP containing composites were recorded as 5.01, 5.00, 5.08 and 4.54 respectively. Although the addition of β -TCP filler did not significantly affect the biodegradation rate of the PPF/VPES polymer according to gravimetric analysis, the presence of β -TCP decreased the acidity of the medium after degradation. The pH - time profiles of the 5, 10 and 15 percent β -TCP composites were similar to each other and the pH values of the medium increased to similar extent as compared to the PPF/VPES polymer, the pH of the 20 percent β -TCP composite on the other hand increased to less extent as compared to the PPF/VPES polymer.

According to an *in-vitro* degradation study of PPF polymer cured with polypropylene fumarate-diacrylate (PPF-DA) macromer, it has been reported that the *in-vitro* degradation rate of PPF/PPF-DA network can be controlled with cross-link density and that the lower pH and addition of β -TCP filler increased the degradation rate. In addition, the release of acid into the medium due to degradation of PPF/PPF-DA structure caused only a minor pH drop (when PPF/PPF-DA double bond ratio was 0.5, pH decreased by 0.1 in 45 weeks, and stayed constant till 52nd week. For the higher PPF/PPF-DA double bond ratios, pH decreased by 0.18 at the end of 52 weeks). And for the 33 percent β -TCP containing PPF/PPF-DA composite, no significant change occurred in the pH of the medium in 52 weeks in spite of the increase in degradation rate with the addition of β -TCP [8].

In the PPF/VPES system, the significant decrease in pH in the first 7 days (Figure 4.15) can be explained by the release of poly(diethyl vinyl phosphonate) (PVPES), which is

believed to form during the cure reactions and which could not join into network structure. Afterwards, pH drop of PPF/VPES material from 7th day to 84th day was recorded as 0.75. The drop in pH from 7th day to 84th day for the 5-10-15 percent β -TCP containing composites were in the range of 0.38-0.48 and that of 20 percent β -TCP containing composite was 0.65. Thus, pH drop between 7th and 84th day was assigned to the degradation of the PPF/VPES network structure. The above mentioned study on the other hand, includes curing of PPF with another prepolymer: PPF-DA, thus no significant pH drop was observed initially due to co-monomer release and as the degradation of the network occurred at a slower rate, a lower extent of decrease in pH was observed at the end of 52 weeks. With the addition of 33 percent β -TCP filler, this decrease in pH was diminished. In our study the the addition of 5-20 percent β -TCP caused the pH of the medium to decrease at a slower rate as compared to the PPF/VPES matrix. If the the fact that the presence of 5-20 percent β -TCP did not cause a significant change in the biodegradation rate according to gravimetric analysis, the obtained result can be explained by the neutralization of H^+ ions or acid in the medium by the phosphate groups of β -TCP.

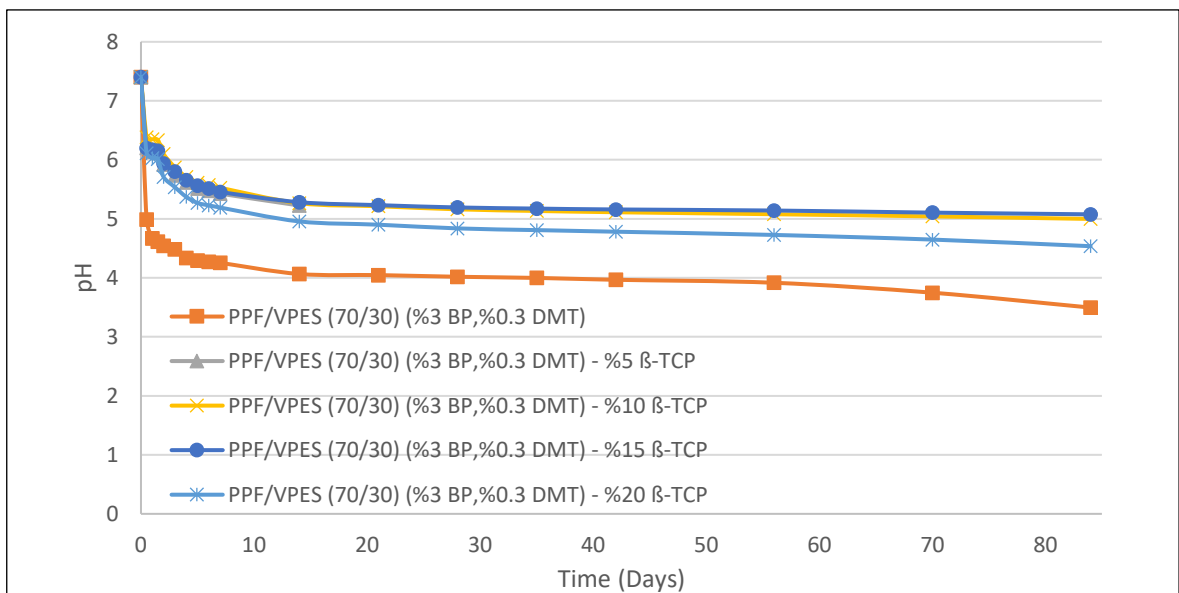


Figure 4.15. pH track of body temperature cured PPF/VPES polymer and PPF/VPES/ β -TCP composites in PBS buffer solution (pH=7.4) at 37 °C.

5. CONCLUSIONS AND FUTURE WORK

5.1. CONCLUSIONS

Poly(propylene fumarate) (PPF) and vinyl phosphonic acid diethyl ester (VPES) based polymeric composites reinforced with Beta-tricalcium phosphate (β -TCP) which were designed to be used as scaffolds for bone tissue defects were developed in this study [48,49]. For this purpose, PPF was synthesized in two molecular weights, as low molecular weight (LMW) PPF (M_n : 1190 g/mol) and high molecular weight (HMW) PPF (M_n : 2558 g/mol). As a result of the optimization studies, HMW-PPF pre-polymer was cured with the VPES comonomer with a fixed PPF:VPES weight ratio of 70:30, in the presence of varying amounts of Beta-tricalcium phosphate (0-20wt percent β -TCP) as filler via radical polymerization using 3 weight percent benzoyl peroxide (BP) initiator and 0.3 weight percent N,N-Dimethyl para-toluidine (DMT) catalyst at 37°C to form biodegradable and biocompatible composite materials that are intended to be used as a bone cement in injectable form. The DSC analysis of the body temperature cured PPF/VPES polymer and PPF/VPES/ β -TCP composites indicated that the cure of these formulations at 37°C were complete. The thermal gravimetric analysis (TGA) of the PPF/VPES/ β -TCP composites showed a one-step degradation of the PPF/VPES network at 290-330°C temperature range and that the char yield at 800 °C increased with increasing β -TCP content indicating the successful integration of the filler material in the composites. Cross-link density of the PPF/VPES matrix decreased with increasing β -TCP amount for the composites. SEM analysis of the fracture surfaces of the PPF/VPES/ β -TCP composites showed that the β -TCP particles were well dispersed on the matrix at 10-20 percent β -TCP content although some aggregate formation was also observed especially for the 15 and 20 percent β -TCP composites. Equilibrium water content (EWC) values of the 5, 10 and 15 wt percent β -TCP composites decreased as compared to that of PPF/VPES matrix which is in favor of dimensional stability of the composites and increased for the 20wt percent β -TCP composite as compared to the PPF/VPES polymer. Surface contact angle with water decreased and therefore surface hydrophilicity of the composites increased with increasing β -TCP content which was in favor of cell viability. The LMW - PPF on the other hand was

able to cure with VPES (PPF:VPES=70:30) completely to a solidified form when a high temperature cure cycle (2 hours at 65°C, 2 hours at 85 °C , 5 hours at 100°C) was applied, therefore high temperature cured PPF/VPES/ β -TCP composites were also prepared with 4, 6, 8, 10, 12, 15wt percent β -TCP using 2 wt percent BP initiator to only demonstrate the cure of these resins at the higher temperature and the potential use of the composites in preformed forms as bone tissue scaffolds. Only DSC analysis of these composites were presented to confirm the successful cure of the formulations applying the high temperature cure conditions.

The compressive modulus and strength values of the body temperature cured PPF/VPES-5-20 percent β -TCP composites were in the range of 1,45 \pm 0.01 MPa - 4,89 \pm 0.05MPa and 1,03. \pm 0.09MPa - 6,86 \pm 1.02MPa respectively. The maximum compressive modulus was obtained for the 10 percent β -TCP composite and compressive strength exhibited the maximum values for the 10 and 15 percent β -TCP composites. The compressive modulus and strength values of the PPF/VPES matrix cured at 37°C were considerably decreased when compared to the compressive properties of the PPF/VPES polymer cured applying the higher temperature cure cycle. Thus when the compressive modulus and strength values determined for the body temperature cured composites are considered, it can be proposed that these composites can be used as scaffolds for bone cartilage rather than bone scaffolds. The compressive modulus and strength values of articular bone cartilage tissue have been recorded as 0.005 – 2 MPa and 0.005 – 1 MPa respectively [50,51].

Finally gravimetric analysis for the *in-vitro* biodegradation of the composites in PBS buffer solution (pH=7.4) at 37°C showed a fast weight loss in the first 7 days then a slower weight loss taking place as observed for the PPF/VPES matrix. The addition of 5-20 percent β -TCP to the PPF/VPES polymer did not significantly affect the weight loss profile and therefore the degradation rate. For the analysis of biodegradation of the composites in PBS buffer solution (pH=7.4) at 37°C via pH change, the initial pH value (7.4) for both the PPF/VPES and its β -TCP composites decreased significantly in the first 7 days and then pH was found to decrease at a slower rate. Although gravimetric analysis indicated that the addition of β -TCP did not significantly affect the biodegradation rate of the PPF/VPES polymer, it resulted in decrease of the acidity of the PBS solution medium after degradation which was in favor of cell viability. In addition, a complementary study carried out on these materials for their role in bone regeneration [47], reported that the

body temperature cured PPF/VPES and PPF/VPES- β -TCP composites were biocompatible and promoted HOb cell attachment, proliferation, growth, and differentiation.

As a result, when all these findings are considered, it can be concluded that the body temperature cured, biodegradable and biocompatible PPF/VPES - 10 percent β -TCP composite which can be utilized in an injectable form seems to have the highest potency to be used as a scaffold for cartilage tissue engineering.

5.2. FUTURE WORK

The homogenous dispersion of the filler in the matrix is vital to get the highest improvement in mechanical and other properties for a composite material. Thus one future work for this study can be to decrease the cure time of the composite formulations at 37°C (body temperature) to increase the homogeneity of the composites and achieve a better dispersion of β -TCP filler in the PPF/VPES matrix especially at higher β -TCP contents. This can be achieved by the addition of a cross-linker into a system. Generally, an inert cross-linker should be used in order to maintain the biocompatibility of the materials. Thus, Titanium containing cross-linkers can be favorable in order to decrease the cure time of a biocomposite [52]. Enhancements of mechanical properties are expected with decreasing the cure time. In addition, the characterization of the high temperature cured PPF/VPES/ β -TCP composites can also be carried out to demonstrate their use as scaffolds in bone tissue engineering in preformed forms.

REFERENCES

1. Vacanti CA. The history of tissue engineering. *Journal of Cellular and Molecular Medicine*. 2006;10(3):569–76.
2. Amini AR, Laurencin CT, Nukavarapu SP. Bone tissue engineering: recent advances and challenges. *Critical Reviews in Biomedical Engineering*. 2012;40(5):363–408.
3. Dreifke MB, Ebraheim NA, Jayasuriya AC. Investigation of potential injectable polymeric biomaterials for bone regeneration. *Journal of Biomedical Materials Research - Part A*. 2013;101 A(8):2436–47.
4. Ngiam M, Liao S, Patil AJ, Cheng Z, Chan CK, Ramakrishna S. The fabrication of nano-hydroxyapatite on PLGA and PLGA/collagen nanofibrous composite scaffolds and their effects in osteoblastic behavior for bone tissue engineering. *Bone*. 2009;45(1):4–16.
5. Zhao F, Yin Y, Lu WW, Leong JC, Zhang W, Zhang J, et al. Preparation and histological evaluation of biomimetic three-dimensional hydroxyapatite/chitosan-gelatin network composite scaffolds. *Biomaterials*. 2002;23(15):3227–34.
6. Narbat MK, Orang F, Hashtjin MS, Goudarzi A. Fabrication of porous hydroxyapatite-gelatin composite scaffolds for bone tissue engineering. *Iranian Biomedical Journal*. 2006;10(4):215–23.
7. He S, J. Yaszemski M, Yasko AW, Engel PS, Mikos AG. Injectable biodegradable polymer composites based on poly(propylene fumarate) crosslinked with poly(ethylene glycol)-dimethacrylate. *Biomaterials*. 2000;21(23):2389–94.
8. Timmer MD, Ambrose CG, Mikos AG. In vitro degradation of polymeric networks of poly(propylene fumarate) and the crosslinking macromer poly(propylene fumarate)-diacrylate. *Biomaterials*. 2003;24(4):571–7.
9. Lewandrowski K, Bondre S, DL W, Tomford W, Trantolo D. Improved osteoconduction of cortical bone grafts by biodegradable foam coating. *Biomed Material Engineering*. 1999;9(5):265–75.

10. Can E, Torun Köse G, Cemali G. A tissue scaffold production method. EP3153187A1, 2017.
11. Nguyen TH, Lee BT. In vitro and in vivo studies of rhBMP2-coated PS/PCL fibrous scaffolds for bone regeneration. *Journal of Biomedical Materials Research - Part A*. 2013;101 A(3):797–808.
12. Ghag AK, Gough JE, Downes S. The osteoblast and osteoclast responses to phosphonic acid containing poly(ϵ -caprolactone) electrospun scaffolds. *Biomaterials Science*. 2014;2(2):233–41.
13. Horowitz RA, Mazor ZI V, Foitzik C, Prasad H, Rohrer M, Palti ADY. β -tricalcium phosphate as bone substitute material : *Journal of Osseointegration*. 2010;1(1):77-92.
14. Anne M. Polymer definition and examples 2018 [cited 2019 28 June]. Available from: <https://www.thoughtco.com/definition-of-polymer-605912>
15. Todd A.R. *Polymer Synthesis - Classification*. New York: Clarkson- Clarkson University Press ; 1980.
16. Nitrocellulose - an overview | ScienceDirect Topics. Applied Polymer Science. 2000 [cited 2019 28 June]. Available from: <https://www.sciencedirect.com/topics/chemical-engineering/nitrocellulose>
17. National Science Foundation. Polymer chemistry-classification of polymers. 2000 [cited 2019 28 June]. Available from: <http://faculty.uscupstate.edu/llever/Polymer Resources/Classification.htm#thermoplastics>
18. Encyclopædia Britannica inc. Chemistry of industrial polymers. 2008 [cited 2019 28 June]. Available from: <https://www.britannica.com/topic/industrial-polymer-chemistry-468716#ref608559>
19. Marmon Aerospace & Defense L. Cross linked polymer | polymer crosslinking | cross linking polymers. 2016 [cited 2019 28 June]. Available from: <http://www.marmon-ad.com/polymer-cross-linking>
20. Basic Polymer Structure | MATSE 81: Materials in today's world [cited 2019 24 July]. Available from: <https://www.e-education.psu.edu/matse81/node/2210>

21. Groover MP. *Fundamentals of modern manufacturing*. California: World Color-John Wiley Press; 2002.
22. Encyclopædia Britannica inc. Polymerization, 2016 [cited 2019 25 July]; Available from: <https://www.britannica.com/science/polymerization>
23. Step-growth polymerization, 2019 [cited 2019 28 June]. Available from: https://polymerdatabase.com/polymer_chemistry/Stepgrowth_Polymerization.html
24. Crystallinity 2000 [cited 2019 28 June]. Available from: http://faculty.uscupstate.edu/llever/Polymer_Resources/Crystalline.htm
25. Hayashi T. Biodegradable polymers for biomedical uses. *Progress in Polymer Science*. 1994;19(4):663–702.
26. Ashammakhi N, Rokkanen P. Absorbable polyglycolide devices in trauma and bone surgery. *Biomaterials*. 1997;18(1):3–9.
27. Yaszemski MJ, Payne RG, Hayes WC, Langer R, Mikos AG. Evolution of bone transplantation: Molecular, cellular and tissue strategies to engineer human bone. *Biomaterials*. 1996;17(2):175–85.
28. Hubbell JA. Biomaterials in tissue engineering. *Bio/Technology*. [cited 2019 30 June] 1995 Jun 1;13:565. Available from: <http://dx.doi.org/10.1038/nbt0695-565>
29. Mikos AG, Temenoff JS. Formation of highly porous biodegradable scaffolds for tissue engineering. *Electronic Journal of Biotechnology*. 2000;3(2):114–9.
30. Gunatillake PA, Adhikari R, Gadegaard N. Biodegradable synthetic polymers for tissue engineering. *European Cells and Materials*. 2003;5:1–16.
31. Nelson CJ, Avgeropoulos GN, Weissert FC, Böhm GGA. The relationship between rheology, morphology and physical properties in heterogeneous blends. *Die Angewandte Makromolekulare Chemie*. 1977;60(1):49–86.
32. Schakenraad J, Nieuwenhuis P, Molenaar I, Helder J, Dijkstra P, Feijen J. In vivo and in vitro degradation of glycine/DL-lactic acid copolymers. *Journal of Biomedical Materials Research*. 1989;23(11):1271–88.

33. Verheyen CCPM, de Wijn JR, van Blitterswijk CA, de Groot K, Rozing PM. Hydroxylapatite/poly(L-lactide) composites: An animal study on push-out strengths and interface histology. *Journal of Biomedical Materials Research*. 1993;27(4):433–44.
34. Diez-Pascual AM. Tissue engineering bionanocomposites based on poly(propylene fumarate). *Polymers*. 2017;9(7):1–19.
35. Lee KW, Wang S, Yaszemski MJ, Lu L. Physical properties and cellular responses to crosslinkable poly(propylene fumarate)/hydroxyapatite nanocomposites. *Biomaterials*. 2008;29(19):2839–48.
36. Mitha MK, Jayabalan M. Studies on biodegradable and crosslinkable poly(castor oil fumarate)/poly(propylene fumarate) composite adhesive as a potential injectable biomaterial. *Journal of Materials Science: Materials in Medicine*. 2009;20:203–211.
37. Alge DL, Bennett J, Treasure T, Voytik-Harbin S, Goebel WS, Chu TMG. Poly(propylene fumarate) reinforced dicalcium phosphate dihydrate cement composites for bone tissue engineering. *Journal of Biomedical Materials Research - Part-A*. 2012;100 A(7):1792–802.
38. Wu SC, Hsu HC, Hsu SK, Wang WH, Ho WF. Preparation and characterization of four different compositions of calcium phosphate scaffolds for bone tissue engineering. *Materials Characterization*. 2011;62(5):526–34.
39. Cai ZY, Yang DA, Zhang N, Ji CG, Zhu L, Zhang T. Poly(propylene fumarate)/(calcium sulphate/ β -tricalcium phosphate) composites: Preparation, characterization and in vitro degradation. *Acta Biomaterialia*. 2009;5(2):628–35.
40. Shalumon KT, Jayabalan M. Studies on biodegradation of crosslinked hydroxy terminated-poly(propylene fumarate) and formation of scaffold for orthopedic applications. *Journal of Materials Science: Materials in Medicine*. 2009;20.
41. Diez-Pascual AM., Diez-Vicente AL. Polypropylene fumarate (PPF): Synthesis and Characterization. *Journal of the Royal Society of Chemistry*. 2017;6(5):1–3.
42. Wang S, Lu L, Yaszemski MJ. Bone Tissue-Engineering Material poly(propylene fumarate): Correlation between molecular weight, chain dimensions, and physical

- properties. *Biomacromolecules*. 2006;71(2):233–6.
43. Ferri JM, Gisbert I, García-Sanoguera D, Reig MJ, Balart R. The effect of beta-tricalcium phosphate on mechanical and thermal performances of poly(lactic acid). *Journal of Composite Materials*. 2016;50(30):4189–98.
 44. Jayabalan M. Studies on Poly(propylene fumarate-co-caprolactone diol) thermoset composites towards the development of biodegradable bone fixation devices. *International Journal of Biomaterials*. 2009;2009(6):1–10.
 45. Jayabalan M, Shalumon KT, Mitha MK, Ganesan K, Epple M. The effect of radiation processing and filler morphology on the biomechanical stability of a thermoset polyester composite. *Biomedical Materials*. 2010;5(2).
 46. Torun Köse G, Korkusuz F, Korkusuz P, Purali N, Özkul A, Hasirci V. Bone generation on PHBV matrices: An in vitro study. *Biomaterials*. 2003;24(27):4999–5007.
 47. Okutan B. Role of poly (Propylene fumarate)(PPF) based scaffolds in bone regeneration. *Yeditepe University*; 2018.
 48. Aruh A, Cemali G, Torun Köse G, Can E. Poli (propilen fumarat) (PPF) bazlı kompozit kemik doku iskelelerinin hazırlanışı ve karakterizasyonu. *Acıbadem Üniversitesi, Biomed Ulusal 23. Bilim ve Teknoloji Sempozyumu*; 2018.
 49. Aruh A, Cemali G, Torun Köse G, Can E. Poly(Propylene Fumarate) (PPF) based composites as scaffolds for bone tissue engineering. *Kimya Mühendisleri Odası, 5. Uluslararası Polimerik Kompozit Sempozyumu*, Izmir, 2018
 50. Boschetti F, Pennati G, Gervaso F, Peretti GM, Dubini G. Biomechanical properties of human articular cartilage under compressive loads. *Biorheology*. 2004;41(3–4):159–66.
 51. Wang CCB, Deng JM, Ateshian GA, Hung CT. An automated approach for direct measurement of two-dimensional strain distributions within articular cartilage under unconfined compression. *Journal of Biomechanical Engineering*. 2002;124(5):557.
 52. Borisov SN. *Organosilicon heteropolymers and heterocompounds*. New York: Springer-Science and Business Media; 2012.

APPENDIX A: DATA OBTAINED FOR CHARACTERIZATION OF PPF/VPES POLYMER AND PPF/VPES/ β -TCP COMPOSITES

Table A.1. Cross-link density and molecular weight between cross-links (M_c) values of body temperature (37 °C) cured PPF/VPES polymer and PPF/VPES/ β -TCP composites

Sample	Cross-link density (mol/cm ³)	M_c (g)
PPF/VPES(70/30) (3% BP, 0.3% DMT)	$8.5 \times 10^{-3} \pm 3.4 \times 10^{-4}$	117.19 ± 4.85
PPF/VPES(70/30) (3% BP, 0.3% DMT)-5% β -TCP	$5.4 \times 10^{-3} \pm 3.7 \times 10^{-4}$	186.27 ± 13.65
PPF/VPES(70/30) (3% BP, 0.3% DMT)-10% β -TCP	$5.1 \times 10^{-3} \pm 8.9 \times 10^{-4}$	196.52 ± 29.24
PPF/VPES(70/30) (3% BP, 0.3% DMT)-15% β -TCP	$4.0 \times 10^{-3} \pm 4.7 \times 10^{-4}$	249.15 ± 26.06
PPF/VPES(70/30) (3% BP, 0.3% DMT)-20% β -TCP	$4.8 \times 10^{-3} \pm 6.1 \times 10^{-4}$	209.98 ± 23.67

Table A.2. Equilibrium water content values of body temperature cured PPF/VPES polymer and PPF/VPES/ β -TCP composites

Sample	Equilibrium Water Content (%)
PPF/VPES(70/30) (3% BP, 0.3% DMT)	17.42 ± 3.62
PPF/VPES(70/30) (3% BP, 0.3% DMT)-5% β -TCP	13.90 ± 1.76
PPF/VPES(70/30) (3% BP, 0.3% DMT)-10% β -TCP	14.48 ± 2.51
PPF/VPES(70/30) (3% BP, 0.3% DMT)-15% β -TCP	14.94 ± 0.20
PPF/VPES(70/30) (3% BP, 0.3% DMT)-20% β -TCP	20.77 ± 4.98

Table A.3. Contact angle with water for the body temperature cured PPF/VPES polymer and PPF/VPES/ β -TCP composites at 30th second

Material	Mean Contact Angle (30 th Second) (°)
PPF/VPES (70/30) (3% BP, 0.3 % DMT)	59.6±1.2
PPF/VPES (70/30)(3% BP, 0.3% DMT) – 5% β -TCP	58.1±2.4
PPF/VPES (70/30)(3% BP, 0.3% DMT) -10% β -TCP	41.5±4.2
PPF/VPES (70/30)(3% BP, 0.3% DMT) -15% β -TCP	43.6±1.6
PPF/VPES (70/30)(3% BP, 0.3% DMT) -20% β -TCP	41.1±1.0

Table A.4. Compressive modulus and strength values of body temperature cured PPF/VPES polymer and PPF/VPES/ β -TCP composites

Sample	Compressive Modulus (MPa)	Compressive Strength (MPa)
PPF/VPES (70/30) (3% BP, 0.3% DMT)	2.32±0.05	3.44±0.68
PPF/VPES (70/30) (3% BP, 0.3% DMT)- 5% β -TCP	3.36±0.31	1.03±0.09
PPF/VPES (70/30) (3% BP, 0.3% DMT) - 10% β -TCP	4.89±0.05	6.7±1.14
PPF/VPES (70/30) (3% BP, 0.3% DMT) – 15% β -TCP	3.89±0.17	6.86±1.02
PPF/VPES (70/30) (3% BP, 0.3% DMT) – 20% β -TCP	1.45±0.01	1.67±0.01